Preparation, characterization and physical properties of new compounds in the system $Ln_2O_3 – ReO_2 – ½ Re_2O_7$ (Ln = lanthanides or yttrium)

Vom Fachbereich Material- und Geowissenschaften
der Technischen Universität Darmstadt

zur
Erlangung des akademischen Grades eines
Dr.-Ing.
genehmigte Dissertation von

Dipl.-Ing. Thomas Hartmann
aus Solingen

Referent:	Prof. Dr. H. Fueß
Koreferent:	Prof. Dr. J. Galy

Tag der Einreichung:	16. Juni 2003
Tag der mündlichen Prüfung:	16. Juli 2003

Darmstadt 2004
D17

Glossary

Symbol	SI	
Å	$1 \cdot 10^{-10}$ m	Angstrom
2θ	°	diffraction angle
h, k, l	-	Miller indices
d	10^{-10} m	d value
f	e / atom	form factor
f', f''	e / atom	anomal dispersion corrections
a, b, c	10^{-10} m	lattice constants
α, β, γ	°	lattice angles
x/a, y/b, z/c	-	atom positions
T	K	temperature
x	mol	moles
g	kg	mass
ρ	g/cm^3	densitiy
M	emu	magnetization
H	G	magnetic field
θ	K	Weiss constant
μ_B	Bohr magnetons	magnetic momentum
C	emu K	Curie constant
C_m	emu g K	Curie constant (mass dep.)
C_χ	emu g G K	Curie constant (mass + field dep.)
V/O	$(10^{-10}$ m$)^3$	volume per oxygen atom

1 Introduction

Rhenium, the 5d element of the manganese group, was discovered in 1925 by Ida and Walter Noddack [1- 3]. Besides other aspects in rhenium chemistry, summarised extensively by Peacock in 1973 [4] and by Rouschias in 1974 [5], several research groups worked on preparation and characterisation of binary and higher rhenium oxides.

In comparison to this rather large number of phases only a small number of ternary oxides in the system $Ln_2O_3 – ReO_2 – ½ Re_2O_7$ (with Ln a lanthanide element or yttrium) have been published, even less have been investigated with respect to their crystal structure, their chemical and physical behaviour. Though all of these rare-earth rhenium oxides are non-metals, isolated metallic Re-Re bonds are typical for most of these compounds with a rhenium oxidation state below +6. Concerning the binary rhenium oxides, ReO_3 shows already metallic behaviour, i.e. Pauli paramagnetism and metallic conductivity. Therefore, rare-earth rhenium oxides might pass from semiconductors to compounds with metallic behaviour for increasing Re-content.

Rare-earth elements are often chosen in structural chemistry because of their ability to vary the electron configurations and magnetic properties in a wide range while keeping nearly the same chemical behaviour in their reactions. Their combination with rhenium to ternary oxides of different stoichiometries should result in an incomparable structural variety.

Some of the already known compounds in the system $Ln_2O_3 – ReO_2 – ½ Re_2O_7$ have only been synthesized with one or at least not all rare-earth elements. A closure of these gaps in the list of known phases is of interest investigating the influence of the respective rare-earth element on the crystal structure and the physical properties of the resulting compound. Yet, the lanthanide contraction with a decrease of the ionic radius from cer to lutetium by approximately 0.15 Å should cause a variation in the structure of the resulting compounds.

Thus the aim of this work has been the search for new phases in the system $Ln_2O_3 – ReO_2 – ½ Re_2O_7$ with a focus on the synthesis of rhenium-rich compounds to check the hypothesis of increasing metallic behaviour due to an increasing Re-content.

2 The system Ln_2O_3 – ReO_2 – ½ Re_2O_7: literature review

In the late nineties of the 20th century only a few phases in the system Ln_2O_3 – ReO_2 – ½ Re_2O_7 (Ln = lanthanide or yttrium) have been known and even less compositions have been confirmed by a complete structure determination.

To give a better impression of the state of the art at the beginning of this thesis a scheme of published phases in the system Ln_2O_3 – ReO_2 – ½ Re_2O_7 is presented in *figure 2.1*.

Broken lines symbolize the oxidation states of rhenium from +4 to +7, lines drawn from the right to the left side of the triangle the Ln : Re ratio from 0 : 1, 1 : 1, 2 :1 to 7 : 1. Each reported stoichiometry is displayed by a circled number. Blue numbers figure compounds with one or more existing structure solution, yellow numbers postulated compositions.

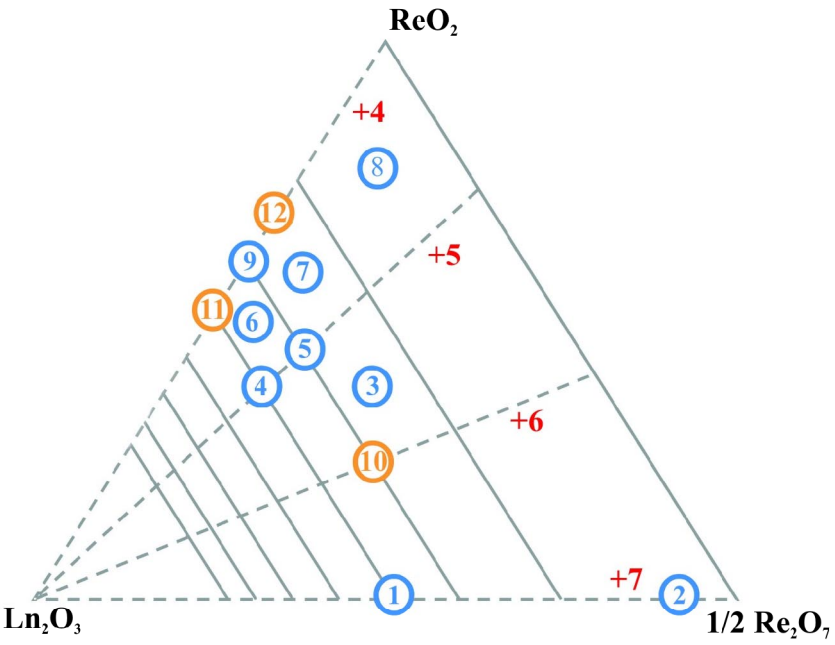

Compound	with Ln =
1: Ln_3ReO_8	Y, La-Lu
2: $Ln(ReO_4)_3$	Y, La-Lu
3: $Ln_3Re_2O_{10}$	La,Pr
4: Ln_3ReO_7	Nd, Pr, Sm
5: $Ln_4Re_2O_{11}$	Pr-Gd
6: $Ln_5Re_2O_{12}$	Y, Dy-Lu
7: $Ln_3Re_2O_9$	La,Pr Nd,Sm
8: $Ln_4Re_6O_{19}$	La-Nd
9: Ln_2ReO_5	Y,La,Nd,Sm-Lu
10: Ln_2ReO_6	La
12: $Ln_6Re_2O_{13}$	Nd,Sm,Gd *
13: $Ln_4Re_3O_{12}$	La,Nd*
	*postulated

Figure 2.1: Scheme of known or postulated phases in the system Ln_2O_3 – ReO_2 – ½ Re_2O_7

The following chapter should give a short description of these phases in the system Ln_2O_3 – ReO_2 – ½ Re_2O_7 separated into binary and ternary oxides, for each in respect to the rhenium oxidation state.

2.1 Binary rhenium oxides in the system Ln_2O_3 – ReO_2 – Re_2O_7

The oxidation state of rhenium in its binary oxides ranges from +3 up to +7. Since the number of structural different rhenium oxides is rather small, no subsections are introduced.

The preparation of rhenium(III)oxide hydrate $Re_2O_3 \cdot H_2O$ was discovered in 1933 by Geilmann and Wrigge [6].

Rhenium(IV)oxide is dimorphous. The preparation of the black ReO_2 has been reported first by Biltz in 1933 [7]. The crystal structure of the monoclinic low-temperature modification, α-ReO_2, has been published in 1957 by Magneli [8]. It is built up by staggered strings of $[ReO_6]$-octahedra as in brookite connected by shared corners as in rutile.
The orthorhombic high-temperature modification β-ReO_2 is formed irreversibly above 733 K from α-ReO_2. The crystal structure of β-ReO_2, as described by Rogers et al. in 1969 [9], is built up by zigzag chains of $[ReO_6]$-octahedra, sharing edges, interconnected by common corners.

In 1932 Biltz, Lehrer and Meisel [10, 11] reported their investigations on the red rhenium(VI)oxide and its structural relation to tungsten(VI)oxide. The solution of the cubic ReO_3-structure similar to the perowskite without the centering atom was published by Sleight and Gilson in 1966 [12] and later confirmed by Dickens and Whittingham in 1968 [13]. Several high pressure modifications have been reported by Jørgensen et al. [14, 15].

In 1968 Krebs solved the structure of the pale yellow, hygroscopic Re_2O_7 which forms double-layers of $[ReO_4]$-tetrahedra sharing corners which are alternatingly connected by $[ReO_6]$-octahedra [16-18].

Re_2O_5 was first mentioned by Walter and Ida Noddack in 1929 as a purplish red compound [2]. Other works from Briscoe et al. (1931) [19], Roth et al. (1932) [20], Meisel (1932) [11] described alternative preparation methods for this red product supposed to be ReO_3 by later publications. Papers from Tribalat et al. (1965) [21] and Borisova et al. (1968) [22] gave reports on a blackish-blue compound with a tetragonal cell, Colaitis et al. (1973) [23] wrote about a monoclinic cell for Re_2O_5, comparable to V_2O_5. However, a conclusive structure solution for the Rhenium(V)oxide is still lacking.

2.2 Ternary oxides in the system Ln_2O_3 – ReO_2 – ½ Re_2O_7

In its ternary oxides rhenium occurs in oxidation states from +4 up to +7 sometimes even in formally broken stoichiometries. Hereby, highest stability is reached in compounds containing Re(+7). Ternary rhenium oxides with a lower oxidation state often disproportionate already under mild conditions yielding a Re(+7) phase. Therefore those few stable oxides in the system Ln_2O_3 – ReO_2 – ½Re_2O_7 with rhenium in an oxidation state lower than +VII are of major interest with respect to their chemical and physical behaviour.

The rhenium atoms in ternary rare-earth rhenium oxides with Re(+6) or Re(+7) appear consequently in an isolated rhenium - oxygen coordination. In compounds with rhenium in formal oxidation states from +5.5 to +4 the rhenium atoms are coordinated to the oxygen atoms by $[Re_2O_{10}]$-units sometimes with Re-Re bonds shorter than those in metallic rhenium (2.76 Å). These $[Re_2O_{10}]$-units are built by $[ReO_6]$-octahedra sharing edges. For an oxidation state of +5 a second rhenium - oxygen coordination polyhedron occurs, $[Re_2O_8]$-units with rhenium coordinated either in squared prisms or squared anti-prisms to the oxygen atoms. *Figure 2.2* represents these different types of Re-O coordination polyhedra.

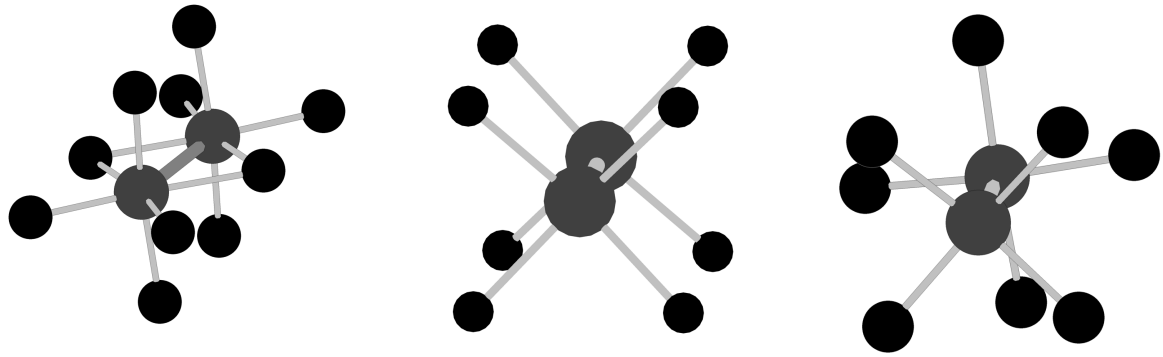

Figure 2.2: Coordination polyhedra with Re-Re bonds: left $[Re_2O_{10}]$-double octahedra, middle $[Re_2O_8]$-squared prism, right $[Re_2O_8]$-squared anti-prism.

In the following part a closer look on the crystal structures of the published rare-earth rhenium oxides shown in the diagram of known phases of the system Ln_2O_3 – ReO_2 – ½Re_2O_7 (*Figure 2.1*) will be given in the order of decreasing oxidation state of rhenium.

2.2.1 Rhenium(+7)

For Re(+7) the most frequently discussed compounds in the system Ln_2O_3 – ReO_2 – ½Re_2O_7 are the rare-earth perrhenates $Ln(ReO_4)_3$ (with Ln = lanthanides and Y). Although already discovered as dehydration products of the rare-earth perrhenate hydrates $Ln(ReO_4)_3 \cdot nH_2O$ (n = 1 to 4) by Varfolomeev and Plyushef in 1966 [24], Khrustalev et al. have published the crystal structure of $Yb(ReO_4)_3$ in 1993 [25]. Rhenium is coordinated to the oxygen atoms by $[ReO_4]$-tetrahedra. Each $[ReO_4]$-tetrahedron is sharing corners with 3-fold capped trigonal $[LnO_9]$-prisms.

Various studies concern rare-earth rhenium oxides Ln_3ReO_8. First published in 1974 by Baud and Besse [26] the structure of the monoclinic Sm_3ReO_8 crystallizes with octahedrally coordinated rhenium atoms and $[Sm_4O]$-tetrahedra which finally has been solved by Besse et al. in 1976 [27].

The crystal structure of La_3ReO_8 has been published in 1979 by Baud et al. and in 1984 by Rae-Smith et al., a report on Y_3ReO_8 was given by Baud et al. in 1981 [28-30]. The cubic, fluorite related structure of Ln_3ReO_8 with Ln = Tb, ..., Lu is also built by $[Ln_4O]$-tetrahedra and an 8-fold coordination of the rhenium atoms by $[ReO_8]$-cubes.

2.2.2 Rhenium(+6)

Only one publication on rare-earth rhenium oxides with rhenium in the oxidation state +6 can be considered as reliable. In 1974 Kurbanov and Mirishli gave a description of the La_2ReO_6 ceramics [31].

Ln_6ReO_{12} compounds had already been proposed in 1964 by Aitken et al. [32] but no successful preparation has been reported.

2.2.3 Rhenium in the formal oxidation state of +5.5

In 1986 Torardi and Sleight [33] published the crystal structure of $La_3Re_2O_{10}$, a ternary rare-earth rhenium oxide with rhenium ions in the formal oxidation state of +5.5. Prepared hydrothermally at 700°C and 0.3 GPa the oxide crystallizes in a monoclinic cell, space group C2/m, with isolated $[Re_2O_{10}]$-units with Re-Re bond lengths of 2.48(1)Å . These $[Re_2O_{10}]$-

units are connected to a three dimensional network by two crystallographically not equivalent lanthanum atoms in an 8-fold coordination. Each Re-Re pair is connected by a σ-bond and one delocalized free electron. As $La_3Re_2O_{10}$ reveals the typical behaviour of a semi-conductor the autors concluded that this electron should remain within the $[Re_2O_{10}]$-unit.

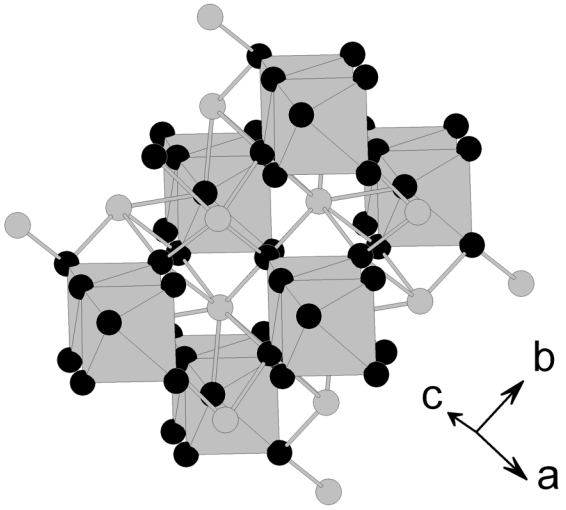

Figure 2.3: Crystal structure of $La_3Re_2O_{10}$, view on the isolated $[Re_2O_{10}]$–double octahedra.

2.2.4 Rhenium(+5)

The same $[Re_2O_{10}]$-units have been found in the crystal structure of $Nd_4Re_2O_{11}$ by Wilhelmi et al. in 1970 [34]. This rare-earth rhenium oxide crystallizes in a tetragonal cell, space group $P4_2/n$, with a Re-Re bond of 2.42(1) Å in the $[Re_2O_{10}]$-units, which are interconnected by $[Nd_4O]$-tetrahedra. Each Nd atom is 8-fold coordinated to oxygen atoms with Re-O bond lengths between 2.32 and 2.55 Å.

Sm_3ReO_7 is the only exception of a rare-earth rhenium oxide with a Re oxidation state <+6 crystallizing in a structure without any Re-Re bonds. The crystal structure was published in 1996 by Wltschek et al. [35] based on an orthorhombic cell, space group Cmcm, with chains of $[ReO_6]$-octahedra sharing corners. These chains are interconnected by samarium atoms in two different coordinations, distorted octahedra or rhombic prisms. Both Sm coordination polyhedra build up chains by sharing edges.

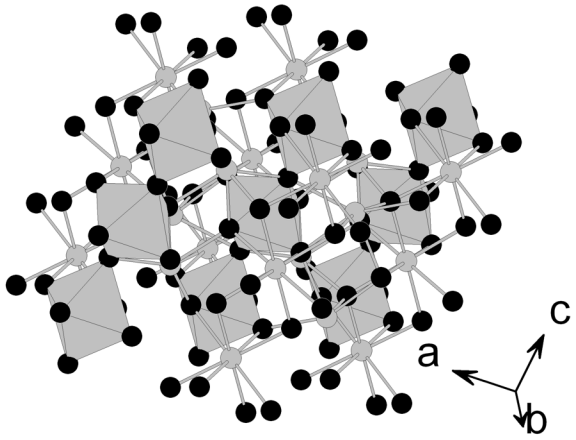

Figure 2.4: Chains of [ReO_6]-octahedra sharing corners.

2.2.5 Rhenium in the formal oxidation state of +4.5 and +4 1/3

Several articles on $Ln_5Re_2O_{12}$ compounds with rhenium in the formal oxidation state of +4.5 have been published but all groups had difficulties in the respective structure solution. In 1977 Savel'eva [36] gave a first description of rare-earth rhenium oxides with the stoichiometry $Ln_5Re_2O_{12}$ for Ln = Y, Dy, ..., Lu. A first structure model for $Dy_5Re_2O_{12}$ was calculated in 1983 by Baud et al. [37] revealing a monoclinic cell, space group $P2_1/m$. Dysprosium atoms are combining planes of [DyO_6]-octahedra-connected chains of [ReO_6]-octahedra to a three dimensional network. Nevertheless, the correct refinement of this structure model failed because of twinning.
A more accurate model, based on a centered monoclinic cell built by chains of distorted [ReO_6]-octahedra with Re-Re bonds of 2.437Å, was published for Ln = Ho by Heumannskämper and Jeitschko in 1987 [38], but all atomic parameters were lacking.

Another rare-earth rhenium oxide with Re(+4.5) is $Ln_3Re_2O_9$, crystallizing in a triclinic cell, space group $P\bar{1}$. Built by isolated [Re_2O_{10}]- and [Re_2O_8]-units the exact stoichiometry should be named $Ln_6[Re_2O_8][Re_2O_{10}]$. This compound was discovered by Besse et al. in 1978 with Ln = La [39], Heumannskämper and Jeitschko had published the isotypic structure of

$Sm_3Re_2O_9$ in 1988 [40]: lanthanide atoms are surrounded by isolated $[Re_2O_{10}]$-double octahedra and squared antiprismatic $[Re_2O_8]$-clusters.

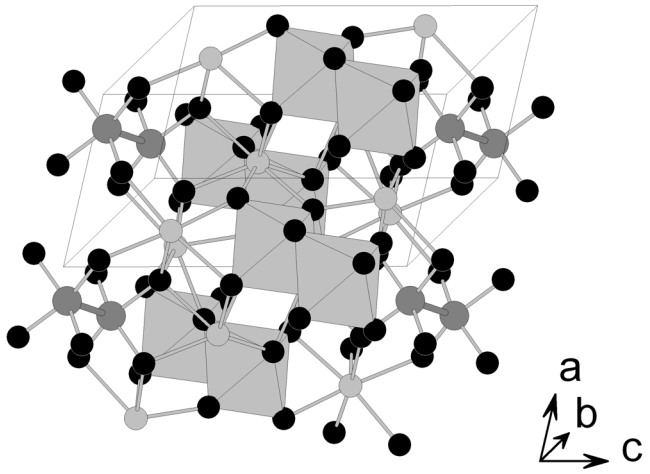

Figure 2.5: $[Re_2O_{10}]$- and eclipsed $[Re_2O_8]$-units in $Sm_3Re_2O_9$.

In 1968 Longo and Sleight [41], Morrow and Katz [42] and Sleight [43] reported independently on $La_4Re_6O_{19}$, a ternary rare-earth rhenium oxide crystallizing in a cubic body-centered cell, space group I23. Its crystal structure is built up by a three dimensional network of $[Re_2O_{10}]$-units with Re-Re bonds of about 2.422Å. Two oxygen atoms of the $[Re_2O_{10}]$-double octahedra point simultaneously to the two outer equatorial atoms of the next $[Re_2O_{10}]$-unit, forming hexagonal channels. Lanthanum atoms 10-fold coordinated in $[La_4O]$-tetrahedra are settled inside these channels. Therefore, the stoichiometry should have been precisely written as $(La_4O) \cdot (Re_6O_{18})$ with rhenium in a formal oxidation state of +4 1/3!

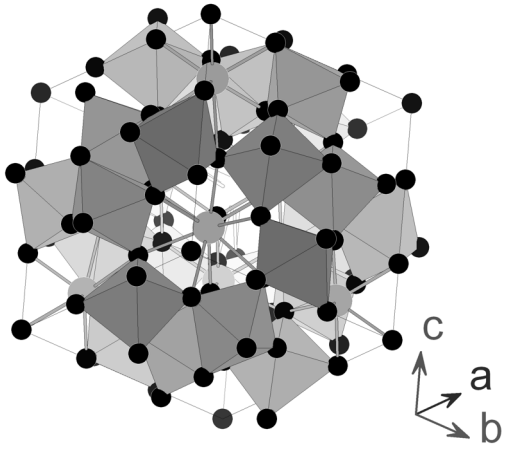

Figure 2.6: View into one of the three hexagonal channels in the unit cell of $Ln_4Re_6O_{19}$.

A more recent work concerning rare-earth rhenium oxides of the composition $Ln_4Re_{5.49}O_{19}$ with Ln = La, Ce, Pr and Nd was published in 1998 by Bramnik et al. [44].

2.2.6 Rhenium(+4)

Reports on compounds with the stoichiometry Ln_2ReO_5 were given by Muller and Roy in 1969 (Ln = Y, Nd, Sm, Gd, Dy, Er and Yb) [45] and Savel'eva et al. in 1977 (Ln = Y, Gd – Lu) [36].
In 1976 Walterson published the structure of La_2ReO_5 [46] which crystallizes in a tetragonal body-centered cell, space group I4/m. The Re^{+4}-ions are four-fold coordinated by oxygen to $[Re_2O_8]$-units building chains along [001].
Heumannskämper and Jeitschko (1988) (Ln = Eu) [40], Wltschek et al. (1997) (Ln = Sm) [47] and Jeitschko et al. again (1999) (Ln = Sm, Eu, Gd) [48] reported about compounds Ln_2ReO_5 crystallizing also in a tetragonal cell, but space group P4/n.

In 2000 Mujica et al. (Ln = Eu) [49] referred to the two different types of $[Re_2O_8]$-units, the tetragonal prismatic and the tetragonal antiprismatic configuration with the oxygen atoms in a staggered or in an eclipsed arrangement with respect to the Re-Re three-fold bond.

Other compounds with rhenium in the formal oxidation state +4 have been published, but are not supported by a structure determination or other results confirming the proposed

stoichiometries. In 1969 Muller and Roy reported on rare-earth rhenium oxides $Ln_6Re_2O_{13}$ with Ln = Nd, Sm and Gd and $Ln_4Re_3O_{12}$ with Ln = Nd [45]. The latter stoichiometry has also been discussed by Baud and Capestan in 1968 with Ln = La [50].

For an overview, all compounds in the system Ln_2O_3 – ReO_2 – ½Re_2O_7 which have already been published at the beginning of this thesis are summarized in *Table 2.1*.

Re oxidation state	Stoichio-metry	Ln	Re-Re unit	Space group	References
+4	Ln_2ReO_5	Y, La, Nd, Sm - Lu	$[Re_2O_8]$	P4/n, I4/m	[40, 45-49]
+4	$Ln_4Re_3O_{12}$	La, Nd			[45, 50]
+4	$Ln_6Re_2O_{13}$	Nd, Sm, Gd			[45]
+4 1/3	$Ln_4Re_6O_{19}$	La - Nd	$[Re_2O_{10}]$	I23	[41-43]
+4.5	$Ln_3Re_2O_9$	La, Pr, Nd, Sm	$[Re_2O_8]$, $[Re_2O_{10}]$	$P\bar{1}$	[39, 40]
+4.5	$Ln_5Re_2O_{12}$	Y, Gd – Lu	$[Re_2O_{10}]$	C2/m	[36-38]
+5	Ln_3ReO_7	Nd, Pr, Sm		Cmcm	[35]
+5	$Ln_4Re_2O_{11}$	Pr - Gd	$[Re_2O_{10}]$	$P4_2/n$	[34]
+5.5	$Ln_3Re_2O_{10}$	La, Pr	$[Re_2O_{10}]$	C2/m	[33]
+6	Ln_2ReO_6	La			[31]
+6	Ln_6ReO_{12}	Ho – Lu		$R\bar{3}$	[53]
+7	$Ln(ReO_4)_3$	Y, La – Lu		$P6_3/m$	[24, 25]
+7	Ln_3ReO_8	Y, La – Lu		$P2_1/a$, $P2_1/m$, $C2_1$, $Fm\bar{3}m$	[26-30]

Table 2.1: Overview on the ternary rare-earth rhenium oxides with respect to their stoichiometry, rare-earth elements, units with metallic Re-Re bonds, space groups and references.

2.3 Previous experiments

Preliminary results have already been obtained by the author and his colleagues before the beginning of this work [51, 52]. Attempting to prepare compounds of the stoichiometry Ln_4ReO_8 with Ln = Gd – Lu by heating mixtures of the respective lanthanide sesqui-oxides and ReO_2 in the ratio of 2 : 1 at 1473 K for 30 h led to compounds $Ln_8Re_2O_{19}$ (Ln = Gd and Dy). Annealing for 36 h with a cooling break after 12 h yielded compounds of the type Ln_6ReO_{12} for Ln = Ho – Lu [53].

2.3.1 $(Ln_{0.81}Re_{0.19})_3O_{5.64}$

Described in [51] and [52] as a high temperature phase "HT1" crystallizing in a rhombohedral cell, space group $R\bar{3}m$ and the broken stoichiometry $(Ln_{0.81}Re_{0.19})_3O_{5.64}$, the compounds $(Ln_{0.81}Re_{0.19})_3O_{5.64}$ have rhenium in its highest oxidation state +7 which is a reasonable value for a phase in the system Ln_2O_3 - ReO_2 – ½Re_2O_7 tempered in air at high temperatures. On the other hand, with Re^{7+} and Ln^{3+} sharing the same site randomly, the proposed structure model does not seem to be reliable. Nevertheless, this phase occurs reproducibly when prepared as mentioned above and remains stable at ambient conditions afterwards. A precise structure solution may be obtained from single crystal data but a preparation of a large enough crystal failed until now. Preliminary crystallographic data are given in *table 2.2*, *figure 2.7* presents a powder pattern taken from $(Gd_{0.81}Re_{0.19})_3O_{5.64}$.

Ln	a [Å]	c [Å]
Gd	3.770(1)	9.547(2)
Dy	3.749(3)	9.392(2)

Table 2.2: Lattice constants of $(Ln_{0.81}Re_{0.19})_3O_{5.64}$ (Ln = Gd and Dy)

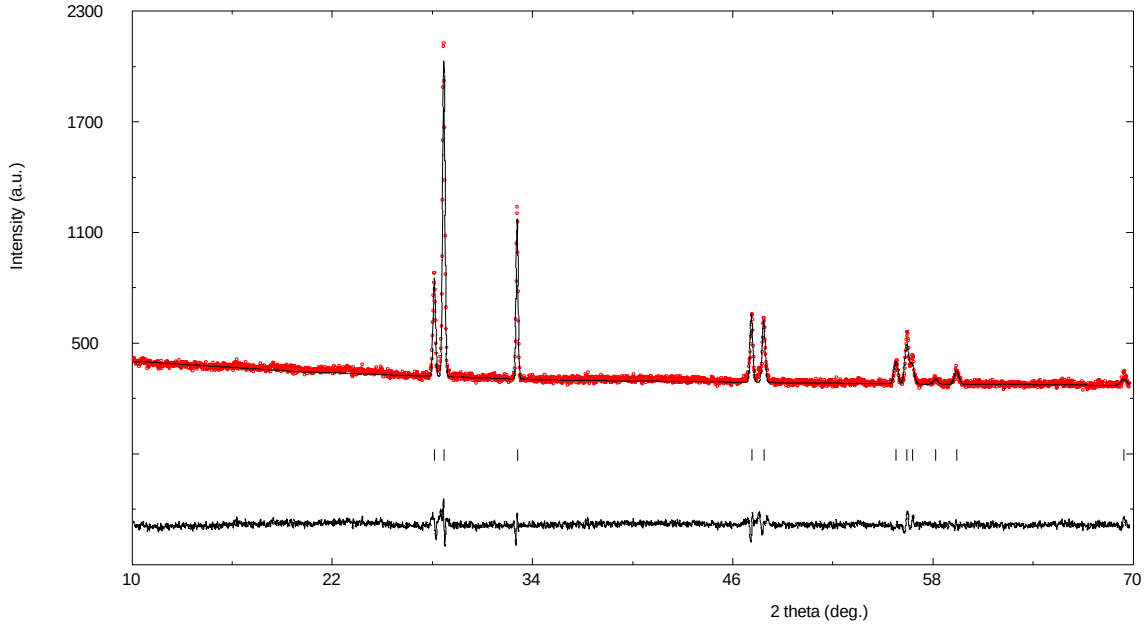

Figure 2.7: Observed and calculated powder pattern of $(Gd_{0.81}Re_{0.19})_3O_{5.64}$ with difference plot and reflection markers from the Rietveld refinement (Cu-Kα_1 radiation).

2.3.2 Ln_6ReO_{12}

The five ternary oxides with the composition Ln_6ReO_{12} have been the first with an accurate structure solution for samples in the system Ln_2O_3 – ReO_2 – ½ Re_2O_7 with rhenium in the oxidation state of +6. They crystallize in a rhombohedral cell, space group $R\bar{3}$. [ReO_6]-octahedra are connected by common oxygen atoms with 12 [LnO_7]-clusters, 6 by sharing edges, 6 by sharing corners (*Figure 2.8*)

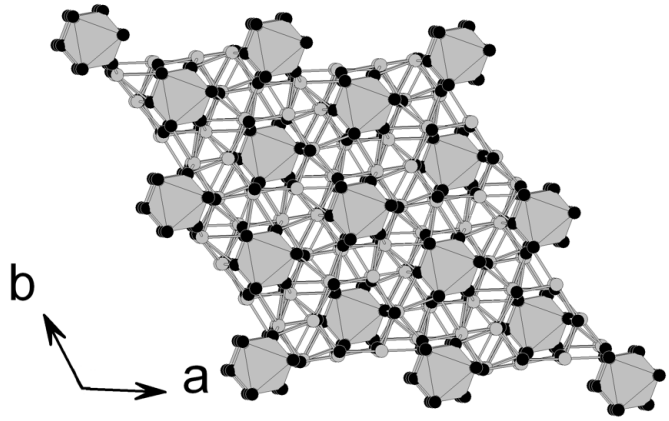

Figure 2.8: Crystal structure of the compounds Ln_6ReO_{12} (Ln = Ho – Lu), view along [100].

The Ln_6ReO_{12} compounds had already been proposed in 1964 by Aitken et al. [32]. They should crystallize in a rhombohedral cell, isostructural to the compounds Ln_6MO_{12} with M = U, Mo and W, respectively, as discovered by Bartram in 1966 [54]. Thus the structure previously proposed has been confirmed with these experiments. The crystallographic data of Tm_6ReO_{12} are given in *table 2.2* as a representative for all Ln_6ReO_{12}.

Atom	Site	x/a	y/b	z/c
Re	3a	0	0	0
Tm	18f	0.2527(3)	0.0411(5)	0.3543(3)
O1	18f	0.185(3)	0.042(4)	0.113(2)
O2	18f	0.226(3)	0.031(4)	0.599(2)

Table 2.2: Positional parameters for Tm_6ReO_{12}.

Except for Lu_6ReO_{12} a deviation from the ideal paramagnetic behaviour at low temperature occurs for all compounds Ln_6ReO_{12}. The inverse magnetisation of Ho_6ReO_{12}, Er_6ReO_{12} and Tm_6ReO_{12} is presented in *figure 2.9*.

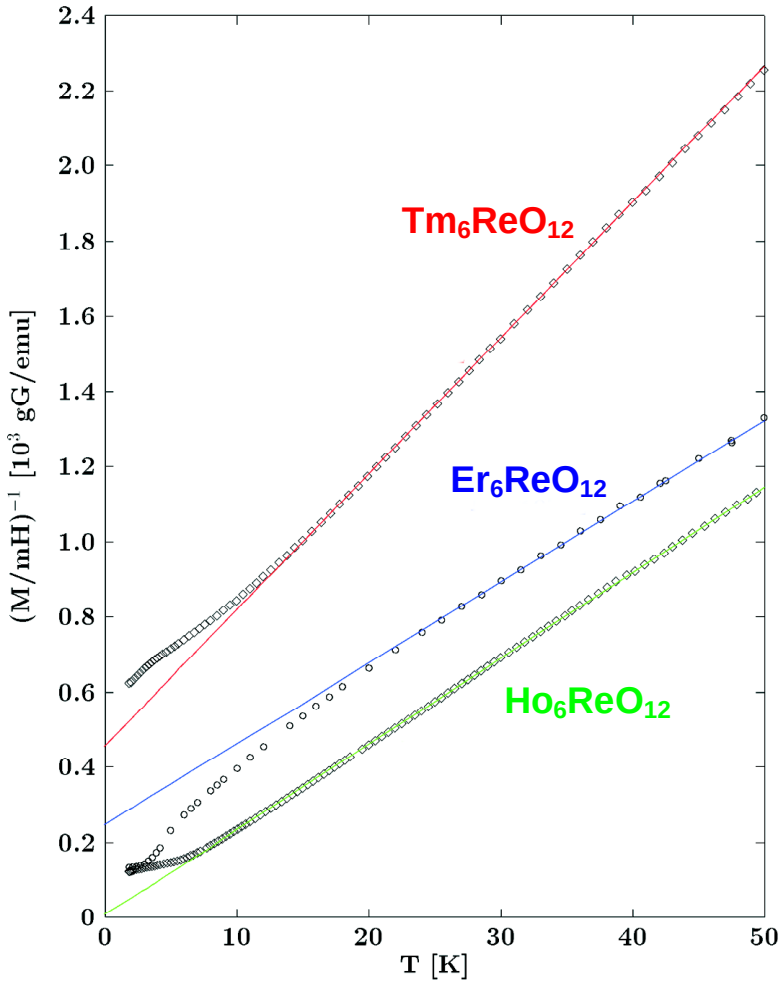

Figure 2.9: Temperature dependent inverse magnetization of Ln_6ReO_{12} (Ln = Ho, Er, Tm). The drawn lines are presenting fits according to the Curie-Weiss law.

The magnetic behaviour of Lu_6ReO_{12} is paramagnetic down to 1.7 K. A modified Curie-Weiss law led to a magnetic moment of 1.5(2) μ_B per Re^{+6} ion.

Every further attempt to prepare compounds of the stoichiometry Ln_4ReO_8 with changes in the temperature program and/or Ln_2O_3 : ReO_2 ratio failed.

3 Preparation and characterization methods

All ternary oxides in the system Ln_2O_3 – ReO_2 – Re_2O_7 have been prepared in a very similar way: Stoichiometric mixtures of the particular rare-earth oxide and rhenium(IV)- and/or rhenium(VI)oxide have been ground under acetone in an agate mortar.
Platinum/rhodium (90/10) tubes (Degussa/Ögussa, specifications see *table 3.1* and *figure 3.1*) were cut into pieces of about 5 cm length and welded electrically at one side. The seam was checked optically for any sign of leakage under a light microscope.

Material	Pt/Rh(90/10%) alloy
Diameter	3.5 mm +/- 0.05 mm
Wall thickness	0.2 mm +/- 0.03 mm
Weight	21 g

Table 3.1: Specifications of the Pt/Rh tubes.

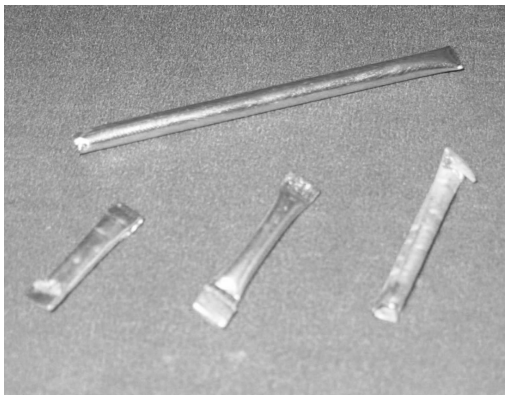

Figure 3.1: Pt/Rh tubes

After drying the mixed compounds were filled into the Pt/Rh (90/10) tubes which have been sealed afterwards by welding, partly in air, partly under argon atmosphere to avoid possible influences of air and moisture on the reaction products.
The sealed Pt/Rh (90/10) tubes were embedded in Al_2O_3 powder filled into a corundum crucible and tempered with various temperature programs in a Gero 70-500 furnace (specifications see *table 3.2*).

After heat treatment the samples have been investigated under a light microscope for optical purity, presence of single crystals and stability.

The used educts are listed with manufacturer and purity in *Table 3.3*.

Type	Gero 70-500 (vertical mounting)
Maximum Temperature	1873 K
Thermocouple	EL 18
Heating rods	3
Material	CrFeAl-alloy
Controller	Eurotherm 818
Tube material	Al_2O_3 (“Pythagoras”)
	gastight, bottom side closed

Table 3.2: Specifications of the Gero furnace.

compound	manufacturer	purity
ReO_2	Strem Chemicals	99.9%
	Aldrich	99.995%
ReO_3	Strem Chemicals	99.9%
	Aldrich	99.9%
Eu_2O_3	Fluka	99.99%
Gd_2O_3	Fluka	99.99%
Tb_2O_3	Strem Chemicals	99.9%
Dy_2O_3	Riedel de Haën	99.99%
Ho_2O_3	Aldrich	99.9%
Er_2O_3	Aldrich	99.99+%
Tm_2O_3	Strem Chemicals	99.9%
Yb_2O_3	Aldrich	99.99%
Lu_2O_3	Aldrich	99.99%
Y_2O_3	Aldrich	99.99%

Table 3.3: Manufacturer and purity of the used educts

A different method has been chosen for the preparation of the binary rhenium oxide Re_3O_{10}. ReO_2 and ReO_3 in ratio 1 : 1 were ground under acetone in an agate mortar and pressed into pellets. These pellets had been heated in a Bühler AM arcmelter afterwards. Further details of this preparation method are given in chapter 6.

Phase analysis was carried out on a STOE STADI P powder diffractometer in transmission mode with a curved position sensitive detector with an angular aperture of 40° in 2θ, measurements for Rietveld refinements on a STADI P with a linear PSD with a 2θ-window of 6°. Further investigations on powder materials have been carried out at the beamline B2, DESY / HASYLAB in Hamburg, Germany, using synchrotron radiation for high-resolution studies.

Single crystals have been measured on a NONIUS CAD4 4-circle diffractometer in kappa geometry, an Oxford Diffraction Xcalibur with CCD detector or at the beamline F1, DESY / HASYLAB, Hamburg, Germany.

Neutron diffraction experiments had been carried out at the ROTAX beamline at the ISIS laboratory in Didcot, UK.

DSC experiments were carried out using a SETARAM DSC 121, DTA/TG investigations on a SETARAM TGA 92.

Transmission electron microscopy investigations have been performed with a Philips CM 20 UT with 200 KV acceleration voltage and a LaB_6 cathode, the image of the $Tm_5Re_2O_{12}$ was obtained using a field emission gun scanning electron microscope Philips XL30 FEG.

4 Re in the formal oxidation state +4.5: $Ln_5Re_2O_{12}$

Except Sm_3ReO_7 all ternary oxides in the system Ln_2O_3 – ReO_2 – ½ Re_2O_7 with rhenium in an oxidation state < +6 show the characteristic $[Re_2O_{10}]$- or $[Re_2O_8]$-units in their crystal structures. This coordination rule has also been valid for all reported structure models of the compounds $Ln_5Re_2O_{12}$ with Ln = Dy [37], Ho [38] and recently for Ln = Y, Gd – Lu (Jeitschko et al., 2000) [55] with chains of distorted $[ReO_6]$-octahedra in different monoclinic cells.

The first exact solution of the crystal structure of the $Ln_5Re_2O_{12}$ is one of the main parts of this thesis and has been determined from a twinned $Tm_5Re_2O_{12}$ crystal by synchrotron diffraction [56].

4.1 Experimental

The samples leading to the structure solution of the $Ln_5Re_2O_{12}$ had been prepared by subsolidus reaction as described in chapter 3 from the rare-earth sesqui-oxides Ln_2O_3 and ReO_2 in ratio 1 : 1. *Table 4.1* represents the details of the synthesis.

Ln	Er, Tm, Ho, Yb, Lu
x(Ln_2O_3)	0.0005 mol
x(ReO_2)	0.0005 mol
Pt/Rh (90/10)-tubes	sealed under Ar-atmosphere
Heating ramp	300 K / h
Reaction temperature	1673 K
Reaction durance	12 h
Cooling ramp	180 K / h

Table 4.1: Preparation details for $Ln_5Re_2O_{12}$.

After opening the Pt/Rh (90/10)-tubes blackish-grey powders with metallic glittering contents trickled out easily. The products have been investigated under a light microscope yielding black, metallic glittering needles (*figure 4.1*) as well as tiny octahedra and grey powder.

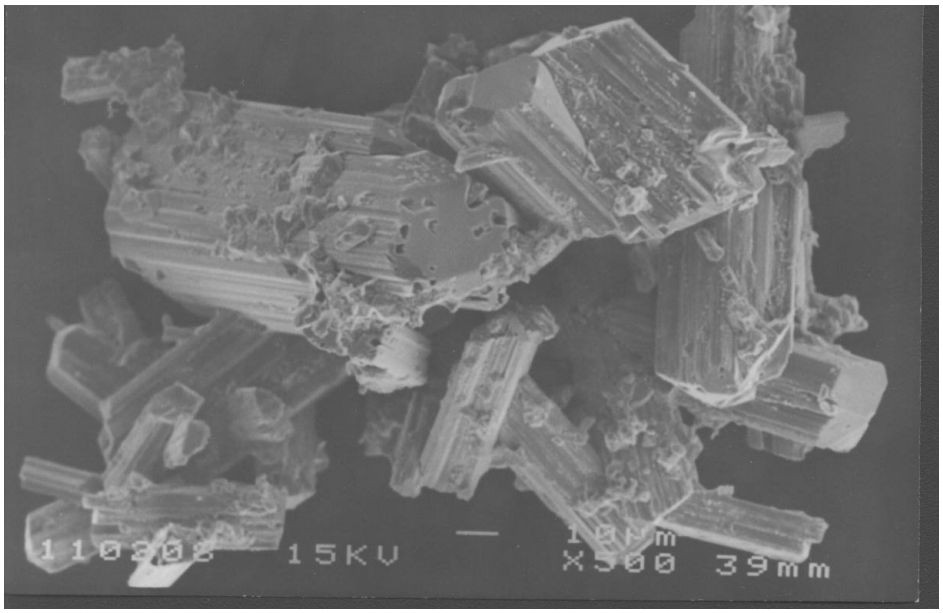

Figure 4.1: Scanning electron micrograph taken from the as synthesized $Tm_5Re_2O_{12}$-sample.

Powder patterns taken from each sample revealed at least two different phases, one of them the cubic, fluorite related Ln_3ReO_8, space group $Fm\bar{3}m$, the second the monoclinic $Ln_5Re_2O_{12}$ phase.

4.2 Structure solution

A needle of approximately 100 µm length and 10 – 15 µm diameter taken from the Tm-sample was isolated and used for diffraction studies. Data collection was performed at the beamline F1, a κ-goniometer with a 1K Smart CCD detector (Bruker/AXS, Karlsruhe), at DESY/HASYLAB, Hamburg, Germany. The incident beam was monochromated by a Si(111) double-crystal monochromator to a wavelength of 0.4275 Å. The beam was unfocused and defined by a slit system to a cross section of 0.12 x 0.12 mm. Its intensity had been monitored by NaI-scintillation counters, a feedback system on the second monochromator crystal ensured constant incident beam intensity.

Several data sets have been collected with a crystal–detector distance of 4 cm with 0.1° rotation per frame and exposure times of 2 and 5 s. The ω scans at six different φ positions in steps of 60° covered 90° in ω, ensuring a coverage of 100% and a redundancy > 12. The integration has been performed with the SAINT program from Bruker/AXS, the absorption correction of the diffracted beam has been calculated by spherical harmonic functions using restrained full-matrix least squares following Blessing's method (1995) [57].

The observed reflections led to structure models with space groups $P2_1/m$ and $P2_1$ and a = 7.4805(4), b = 5.6744(3), c = 12.3717(7) Å and β = 107.816(2)°. However, refinement using both models led to too short Re-O bonds of approximately 1 Å, the reliability values remained at 15%. Therefore and because of unusual extinction rules, all reflections with h even and k + l odd are systematically absent, the possibility of twinning was taken into account.

These extinction rules can be explained by centering and a twinning law based on two domains, linked to each other by a rotation through 180° about the c*-axis. The transformation to the standard setting is reached by interchanging the a and c-axis yielding C symmetry and the lattice parameters a = 12.3717(7), b = 5.6744(3), c = 7.4805(4) Å and β = 107.816(2)°. The refinement of the non-overlapping reflections revealed a ratio of 3.4:1 between domain 1 and 2 which was used for the intensity separation of the overlapping reflections. The set of reflections for the dominant domain with 4961 unique reflections and an R_{int} of 5.32% was used for the structure solution and refinement using SHELXS97 and SHELXL97 (Sheldrick 1990 and 1997) [58, 59].

4.3 Results

The atomic parameters of the refined structure model are listed in *Table 4.2*, the reliability value R_1 has been calculated to 6.82 % for 4165 reflections with $F_o > 4\sigma(F_o)$ and to 8.17 % for all 4961 unique reflections.

Atom	Site	x/a	y/b	z/c	U_{eq}
Re(1)	(4g)	0	0.28367(4)	0	0.00224(3)
Tm(1)	(2d)	½	0	½	0.00381(5)
Tm(2)	(4i)	0.31373(2)	½	0.17505(5)	0.00319(4)
Tm(3)	(4i)	0.19638(2)	0	0.35973(5)	0.00313(4)
O(1)	(4i)	0.0012(4)	0	0.1787(8)	0.0057(5)
O(2)	(4i)	0.4989(5)	0	0.2053(9)	0.0076(6)
O(3)	(8j)	0.3459(3)	0.2520(8)	0.4265(7)	0.0060(4)
O(4)	(8j)	0.1655(3)	0.2461(8)	0.0833(8)	0.0063(4)

Table 4.2: Fractional atomic coordinates and equivalent isotropic displacement parameters ($Å^2$)

The crystal structure of $Tm_5Re_2O_{12}$ is built by chains of distorted [ReO_6]-octahedra sharing edges along [010]. The Re-Re distances are alternating between 2.455(1) and 3.219(1) Å. These chains are interconnected along [001] by [TmO_6]-octahedra via the equatorial O atoms of two [ReO_6]-octahedra of the chain with short Re-Re bonds. The [TmO_6]-octahedra, with Tm(1) by the notation of *Table 4.2*, are not connected to each other, *Figure 4.2* displays this layer.

Tm(2) and Tm(3) have a seven fold oxygen coordination yielding monocapped trigonal [TmO_7]-prisms with O(3) and O(4) forming the prisms and O(1) the capping atom. The prisms for Tm(2) and Tm(3) are differing in the position of O(1) which is shifted from the centre of the capped face leading to elongated edges O(1)-O(3) with 3.361 Å for Tm(2) and 3.296 Å for Tm(3) and shortened O(1)-O(4) bonds of 2.752 Å for Tm(2) and 2.734 Å for Tm(3).

Zigzag chains of either [Tm(2)O_7]- or [Tm(3)O_7]-prisms are running parallel to [010] with the capped face alternating up and down. These chains are connected to each other along [001] by sharing edges O(3)-O(3) or O(4)-O(4). This frame builds a second layer which is shown in *figure 4.3*.

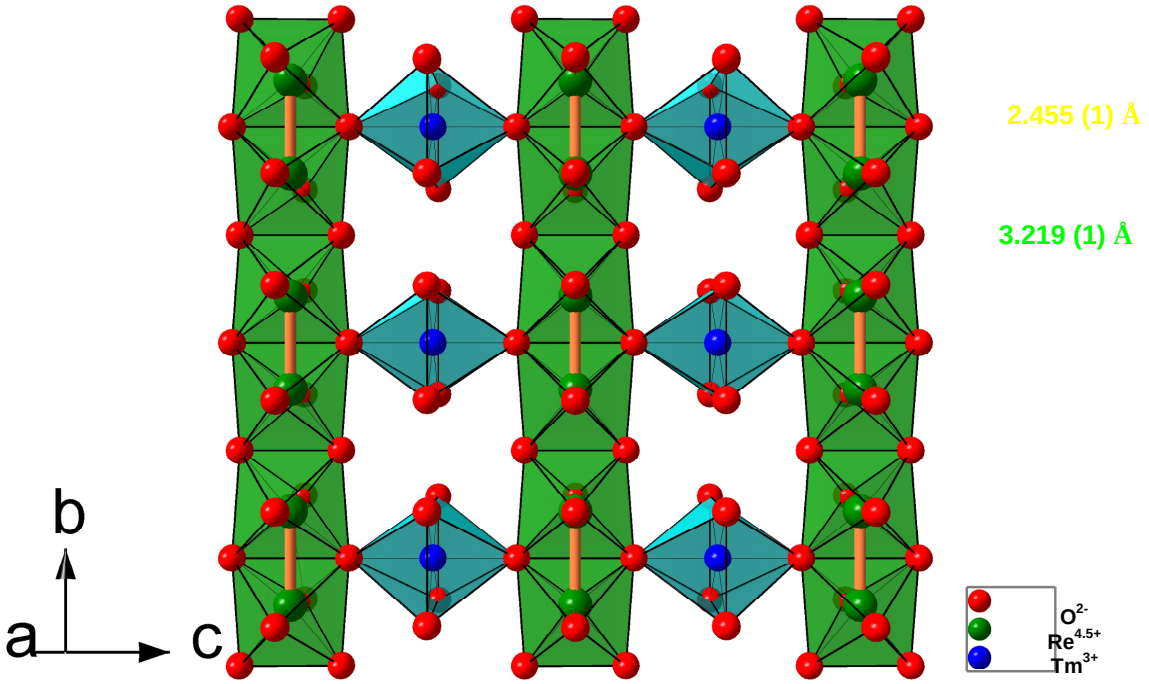

Figure 4.2: Sketch of the [ReO_6]-octahedra chains connected by isolated [$Tm(1)O_6$]-octahedra in $Tm_5Re_2O_{12}$. The lengths of the alternating Re-Re bonds are written in yellow (short) and green (long)..

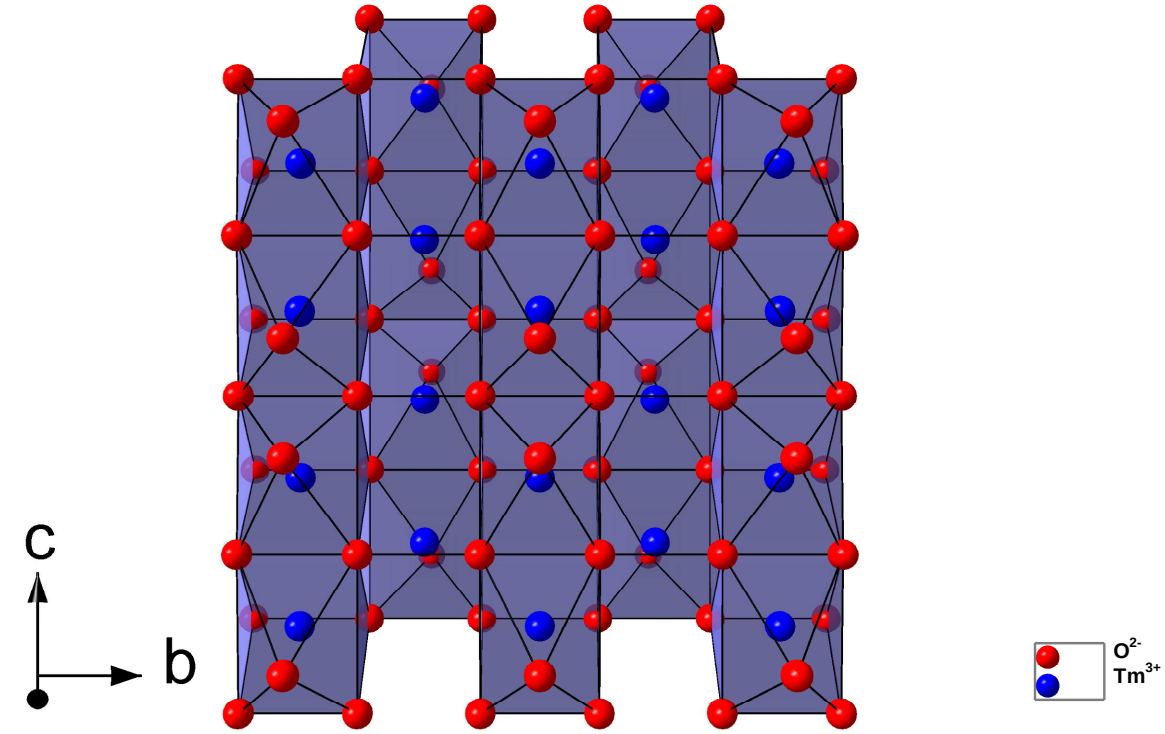

Figure 4.3: Second layer in $Tm_5Re_2O_{12}$, view on the distorted monocapped trigonal prisms.

Both layers are linked to each other building a 3-dimensional network. Each [Tm(2)O_7]-polyhedron is connected to four [ReO_6]-octahedra, to two of them by common edges, to the other two by sharing corners. The [Tm(3)O_7]-prisms are connected with two [ReO_6]- and two [TmO_6]-octahedra, all by sharing edges (*figure 4.4*).

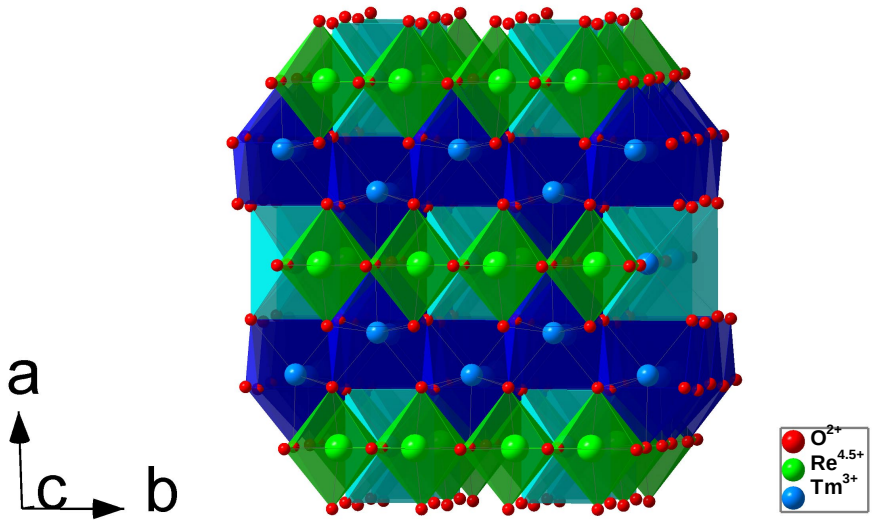

Figure 4.4: Crystal structure of $Tm_5Re_2O_{12}$ with all O-atoms red, [ReO_6]-octahedra green, [Tm(1)O_6]-octahedra cyan and [Tm(2)/Tm(3)O_7]-prisms blue.

These results are in agreement with the structural aspects published for $Ln_5Re_2O_{12}$ compounds by Heumannskämper and Jeitschko preliminary in 1987 (Ln = Ho) [38] and by Jeitschko et al. later in 2000 [52] (Ln = Y, Gd, ..., Lu). An isotypic structure has been published for ternary rare-earth molybdenum oxides $Ln_5Mo_2O_{12}$ (Ln = Y and Gd) by Torardi et al. in 1985 [60].

A small amount of the $Er_5Re_2O_{12}$ sample had been investigated at the beamline B2 at DESY / HASYLAB, Hamburg, by resonant diffraction at the Er L_{III}-edge using an imaging plate detector [61]. Therefore, 10 data sets have been measured at different wavelengths close to the Er L_{III}-absorption edge (8.45 keV). The imaging plate had been read on an external scanner, and the obtained data have been used for Rietveld refinement using the monoclinic cell of $Tm_5Re_2O_{12}$ as the structure model.

The imaging plate data had been of very good quality, so that the thermal displacement parameters could be refined anisotropically after numerical absorption corrections. Resonant diffraction has proved that no Re-atoms occupy Er-sites and vice versa. Furthermore, a very small impurity has been identified as Er_2O_3. The refined values for the dispersion correction terms f' and f" in $f = f_0 + f' + i\,f"$ are shown in *figure 4.5* and are compared with literature data for free Er^{+3}-ions (drawn lines) [62].

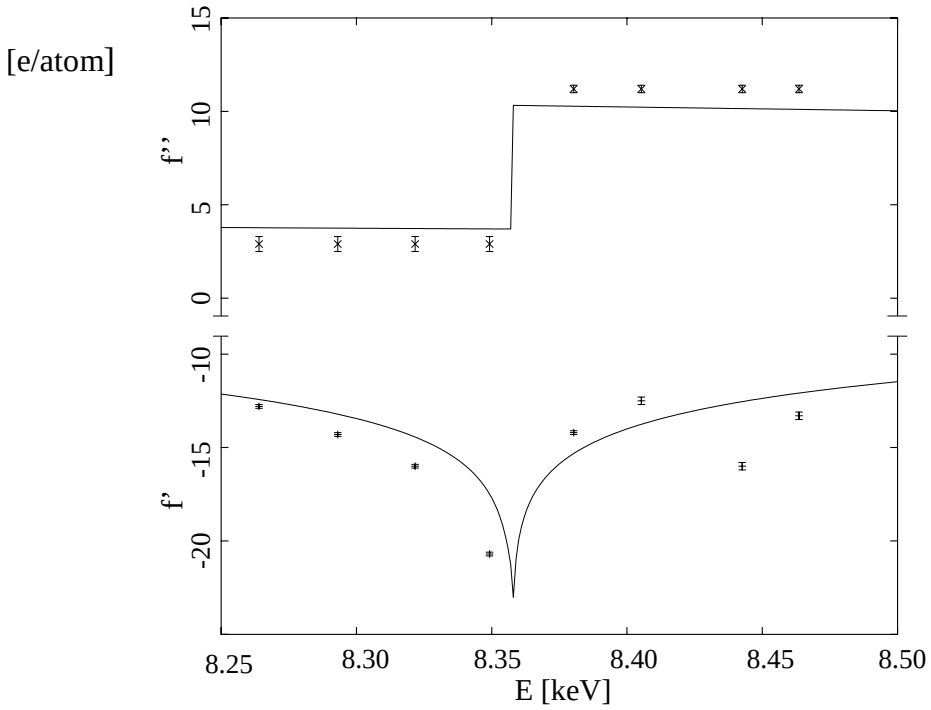

Figure 4.5: Refined and theoretical values for the dispersion corrections f' and f" versus X-ray energy.

Powder data have been measured for all five $Ln_5Re_2O_{12}$ samples with Ln = Er, Ho, Yb and Lu on the STOE STADI P diffractometer. Based on the structure model of $Tm_5Re_2O_{12}$ the crystal structures have been refined by the Rietveld method using the FULLPROF software package [63]. All $Ln_5Re_2O_{12}$ are isotypic, the samples with Ln = Ho, Tm and Lu contained a second phase, which could be identified easily as the cubic fluorite structure of the respective Ln_3ReO_8. *Figure 4.6* displays the powder pattern of the pure Yb-sample as a representative, lattice constants and cell volume for all $Ln_5Re_2O_{12}$ compounds are given in *table 4.4*.

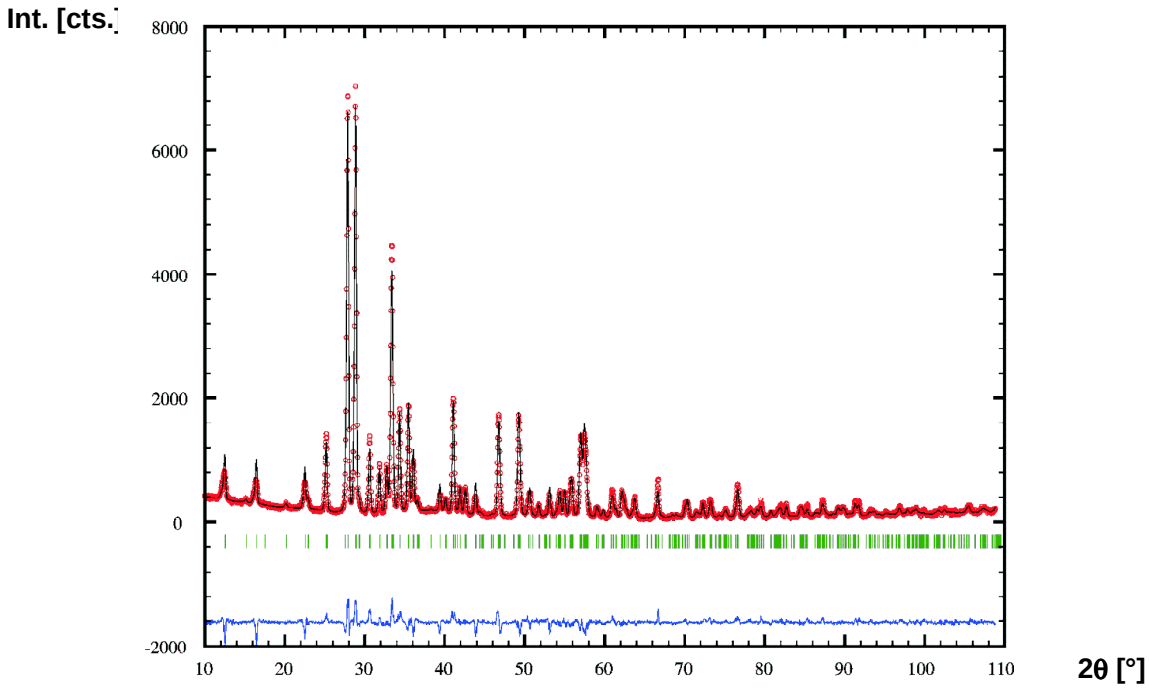

Figure 4.6: Observed and calculated powder pattern taken from the $Yb_5Re_2O_{12}$ sample with difference plot and reflection markers.

Ln	a [Å]	b [Å]	c [Å]	β [°]	Volume [Å^3]
Ho	12.3995(5)	5.6493(2)	7.4906(3)	107.840(3)	499.48(3)
Er	12.3287(5)	5.6285(2)	7.4450(3)	107.837(3)	491.79(3)
Tm	12.2929(7)	5.6168(3)	7.4181(4)	107.823(4)	487.62(4)
Yb	12.2392(9)	5.6063(3)	7.3950(5)	107.797(5)	483.13(5)
Lu	12.2008(9)	5.6042(4)	7.3741(5)	107.764(6)	480.17(6)

Table 4.4: Lattice constants, monoclinic angle and cell volume of all investigated $Ln_5Re_2O_{12}$ compounds.

Taking into account the similarity of the lattice parameters and the proposed centered monoclinic symmetry of the compounds Ln_2ReO_5, Ln = Y, Gd, Dy, Er, Yb, (Muller and Roy, 1969 [45]), it leads to the assumption that those rare-earth rhenium oxides might be in fact of composition $Ln_5Re_2O_{12}$. A comparison of the reflection intensities of a powder pattern taken from "Yb_2ReO_5" and those of $Tm_5Re_2O_{12}$, given in *table 4.5*, supports this assumption strongly.

hkl	Yb_2ReO_5; I/I_{max} [%]	$Tm_5Re_2O_{12}$; I/I_{max} [%]
(001)	4	10
$(20\bar{1})$	5	6
(201)	7	5
(002), $(20\bar{2})$	20	18
(310)	90	100
$(11\bar{2})$	100	98
(400)	21	17
(020)	8	17
(112), $(31\bar{2})$	14	10
$(40\bar{2})$, (202)	84	58
(021)	20	21
(220)	19	31
$(22\bar{1})$	10	12
$(20\bar{3})$	2	2
(221)	3	5
$(22\bar{2})$, (022)	28	33
(510)	9	7
$(51\bar{2})$, (312)	9	8
$(42\bar{1})$	5	6
(600), $(42\bar{2})$, (222)	43	35
$(20\bar{4})$	48	22
(023)	8	6

Table 4.5: Comparison of reflection intensities between Yb_2ReO_5 [45] and $Tm_5Re_2O_{12}$.

Therefore, it is very likely that the proposed compounds Ln_2ReO_5 are in fact $Ln_5Re_2O_{12}$ with its twinned monoclinic structure.

4.4 High temperature experiments

The chains of [ReO_6]-octahedra along [010] with alternating Re-Re distances in the $Ln_5Re_2O_{12}$ structure are close to a one-dimensional conductor. Furthermore, a pseudo symmetry occurs for both layers building the unit cell of these oxides. A two-fold axis perpendicular to the bc-plane is only broken by small structural distortions.
In the light of this pseudo symmetry the twinning appears as a consequence of a phase transition from a higher symmetric high-temperature phase during cooling. The transformation from the monoclinic to this orthorhombic high-temperature cell is given by:

$$\vec{a}_m = \vec{a}_o\,, \qquad \vec{b}_m = \vec{b}_o\,, \qquad 2\vec{c}_m + \vec{a}_m = \vec{c}_o$$

In this case the alternating Re-Re distances can be explained as dimers in result of a Peierls instability of a high-temperature phase with one-dimensional metallic conductivity. Furthermore, $Er_5Re_2O_{12}$ shows an endothermic signal at a temperature around 923 K in a DSC experiment (*figure 4.7*).

In order to prove the existence of this predicted orthorhombic high-temperature phase high-temperature experiments have been carried out at the beamline B2 at DESY/ HASYLAB, Hamburg. A mixture of $Yb_5Re_2O_{12}$ and diamond powder to avoid absorption effects has been sealed in a quartz capillary and measured with a STOE furnace in Debye-Scherrer mode. Due to the recrystallisation point of quartz around 1300 K the measurement had to be stopped at 1273 K without any observed phase transition.
Therefore $Er_5Re_2O_{12}$ has been thinned with corundum powder and afterwards filled in an Al_2O_3-tube which has been sealed with ZrO_2 cement and adjusted in a mirror furnace. This experiment, again at the beamline B2 at DESY/HASYLAB Hamburg, led only to a reaction of the $Er_5Re_2O_{12}$ and the corundum to $Er_3Al_5O_{12}$ [64, 65] with a loss of Re_2O_7. The powder pattern of this phase taken at 1673 K is shown in *figure 4.8*.

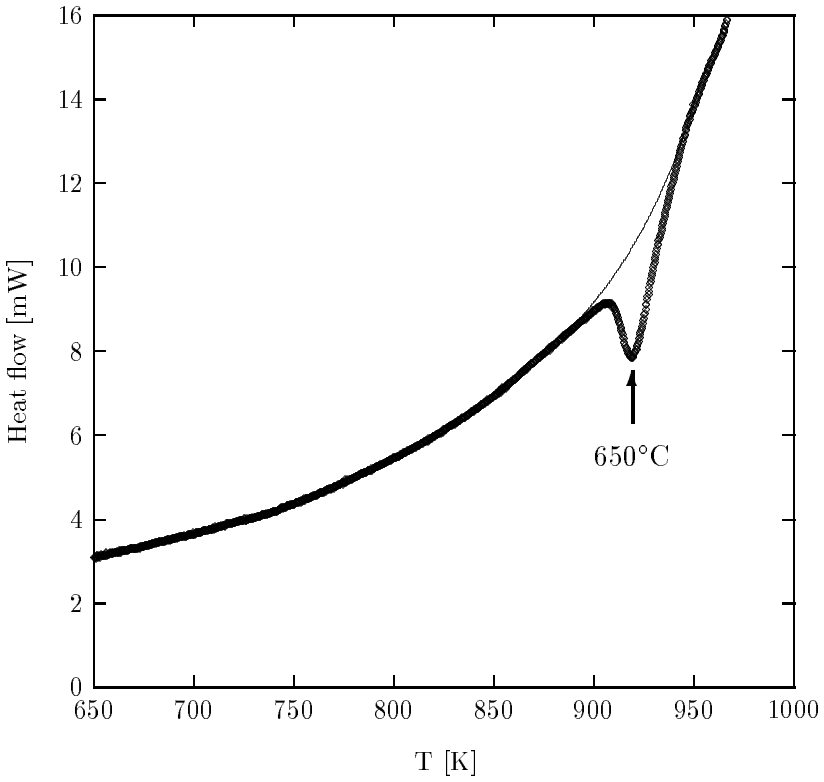

Figure 4.7: DSC measurement of $Er_5Re_2O_{12}$.

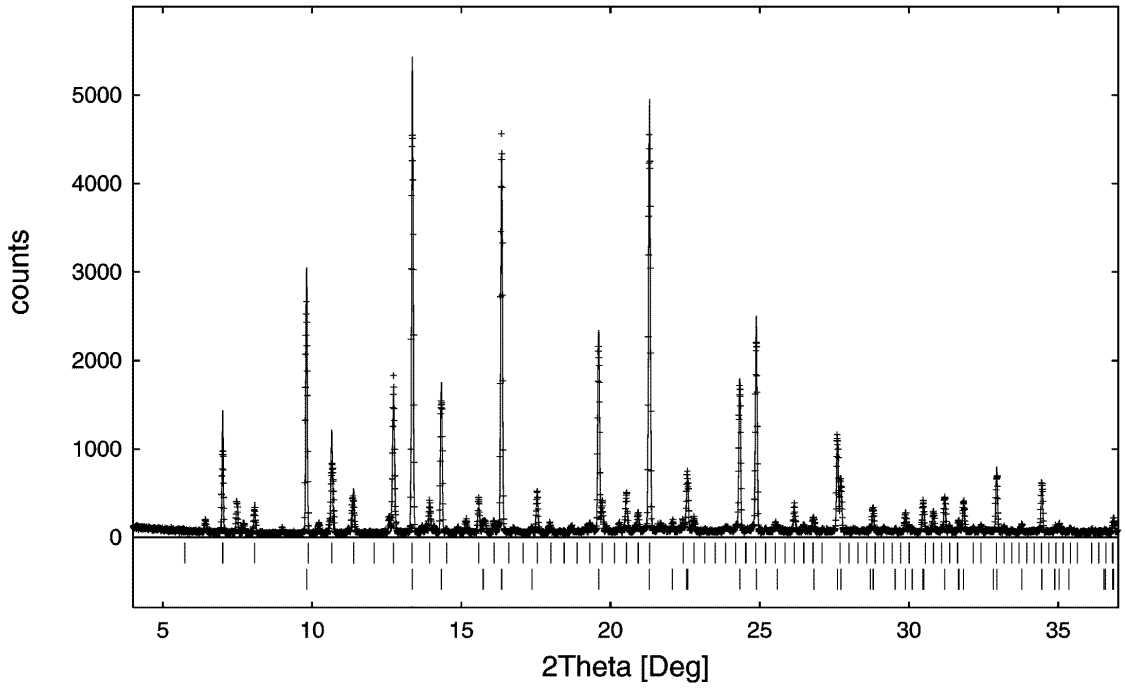

Figure 4.8: Powder pattern taken at 1673 K from a mixture of $Er_5Re_2O_{12}$ and Al_2O_3 in a corundum tube. The material has nearly completely transformed to $Er_3Al_5O_{12}$ (top reflection markers, bottom markers belonging to Al_2O_3). A minor garnet is visible but could not be identified.

4.5 Magnetic properties

Due to the paramagnetic behaviour of $Lu_5Re_2O_{12}$ in a temperature range from 5 to 35 K the magnetic moment of this sample had been calculated to $0.13\mu_B$ per Re-ion, only. Neglecting this rather small part of the Curie constant in $Er_5Re_2O_{12}$ and $Yb_5Re_2O_{12}$ the magnetic moments of Er and Yb have been calculated to $9.73(1)\mu_B$ per Er-ion and $4.1(1)\mu_B$ per Yb-ion. *Figure 4.9* is representing the temperature dependent magnetization of both $Ln_5Re_2O_{12}$-samples. Contrary to the Er-sample $Yb_5Re_2O_{12}$ shows a significant deviation from the Curie-Weiss behaviour already at 100 K.

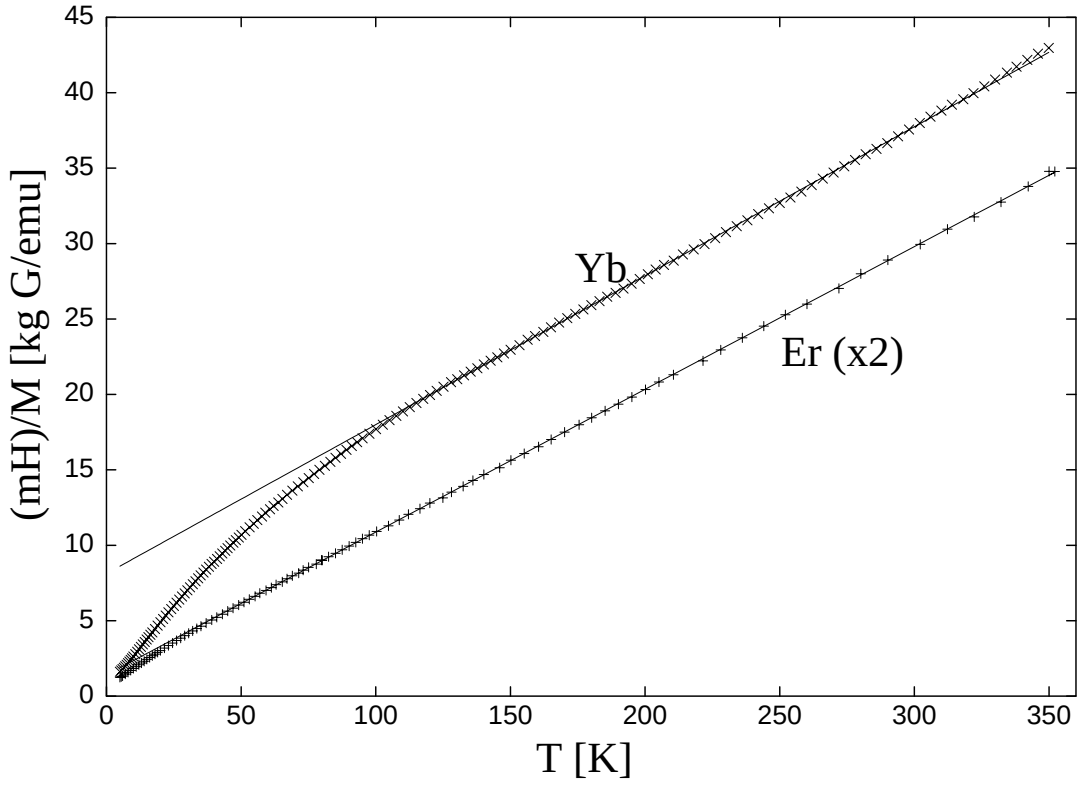

Figure 4.9: Temperature dependence of the inverse magnetization for $Ln_5Re_2O_{12}$ with Ln = Er and Yb. For clarity the values of the $Er_5Re_2O_{12}$-sample have been multiplied by a factor of 2.

5 Compounds related to "Ln_3ReO_8"

Besides the perrhenates $Ln(ReO_4)_3$ only one composition, Ln_3ReO_8, has been reported in the literature with rhenium in its highest oxidation state +7. Accordingly, Ln_3ReO_8 with Ln = Tb – Lu crystallizes in a fluorite-type structure with a random distribution of Ln and Re on one site[26]. For all other rare earth elements with larger ionic radii monoclinic structures are reported [27-30].

The first section of this chapter reports generally on the synthesis of "Ln_3ReO_8" compounds, their magnetic properties and preliminary structural investigations. The proposed fluorite-type structure with Re^{7+} and Ln^{3+}, randomly distributed on one crystallographic site, raises some doubts. There are, at least, three aspects which should favour a more complicated crystal structure with cation ordering:

1. The formal charges +7 and +3 are very different, and a lower electrostatic energy is expected for an ordered arrangement.
2. The ionic radii differ significantly [31], e.g. for coordination number 6 a radius of 0.53 Å is given for Re^{7+} compared to values for the Ln-ions between 0.861 Å for Lu^{3+} and 1.032 Å for La^{3+}.
3. Characteristic coordination polyhedra for Re^{7+} are $[ReO_4]$-tetrahedra and $[ReO_6]$-octahedra, while capped trigonal prisms are the most common coordinations of Ln^{3+}.

In the light of the latter two aspects the proposed $[(Ln,Re)O_8]$-coordination cube in a fluorite-type structure appears very questionable. Therefore, the following sections describe detailed structural investigations by single crystal X-ray diffraction, transmission electron microscopy and synchrotron powder diffraction on selected samples to elucidate even small deviations from fluorite-type patterns and, hereby, to reveal the correct crystal structures of those compounds, previously approximated and summarized as "Ln_3ReO_8".

5.1 Syntheses, magnetic properties and preliminary investigations

In numerous syntheses using the sealed Pt/Rh (90/10)-tubes method with various Ln : Re ratios (Ln = Eu – Lu) and different temperature programs octahedral shaped, metallic black and metallic black crystals appeared barely visible as an additional phase. Powder patterns taken from these reaction products revealed the characteristic reflections of the cubic, fluorite related structure, space group $Fm\bar{3}m$, supposed to be Ln_3ReO_8 [26] and therefore they have not been investigated further for a longer period.

When heating up to temperatures higher than 1773 K pure phases of the composition "Ln_3ReO_8" could be prepared for Ln = Eu, Dy and Y under the conditions listed in *table 5.1*.

Ln	Eu, Dy	Y
x(Ln_2O_3)	0.001 mol	0.001 mol
x(ReO_2)	0.002 mol	0.001 mol
Pt/Rh (90/10)-tubes	sealed under Ar-atmosphere	sealed tubes
Heating ramp	300 K / h	300 K / h
Reaction temperature	1773, 1823 K	1773 K
Reaction durance	24 h	24 h
Cooling ramp	180 K / h	180 K / h

Table 5.1: Reaction conditions of "Ln_3ReO_8" with Ln = Eu, Dy and Y.

As an example, *Figure 5.1* represents a typical observed powder pattern of Dy_3ReO_8 combined with the calculated pattern after Rietveld refinement using the cubic, fluorite related $Fm\bar{3}m$ structure as the model. Reflection markers and the difference plot are included. Re and Dy atoms are sharing the same site (0, 0, 0) the O atoms are located at (¼, ¼, ¼).

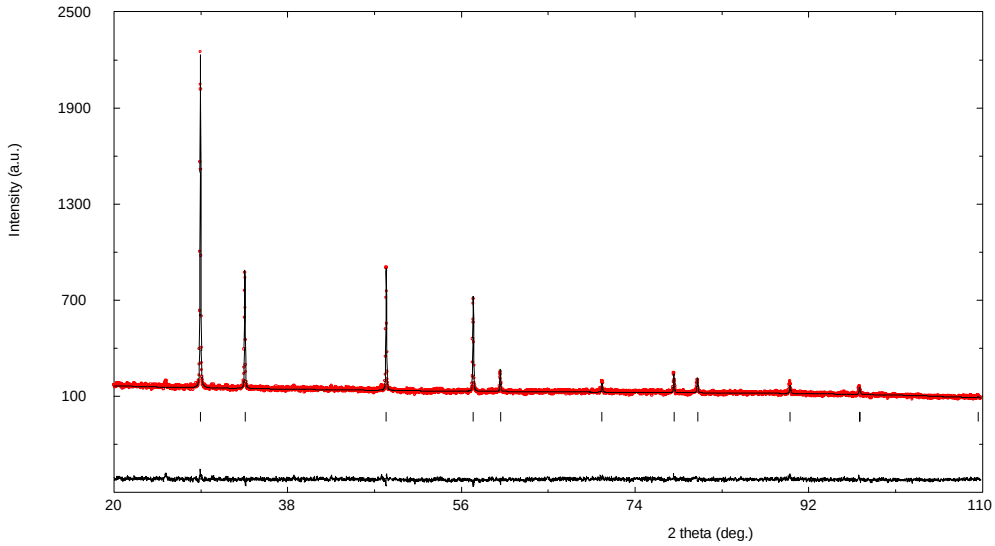

Figure 5.1: Observed and calculated pattern of Dy_3ReO_8 including reflection markers and difference plot of the Rietveld refinement.

Nearly all compounds of the composition Ln_3ReO_8 have paramagnetic behaviour even at very low temperatures and show only small deviation from the Curie-Weiss law. Only Gd_3ReO_8 orders ferromagnetic at temperatures below 10 K. *Figures 5.2* and *5.3* present the temperature dependent inverse magnetization of the "Ln_3ReO_8" with Ln = Gd – Lu.

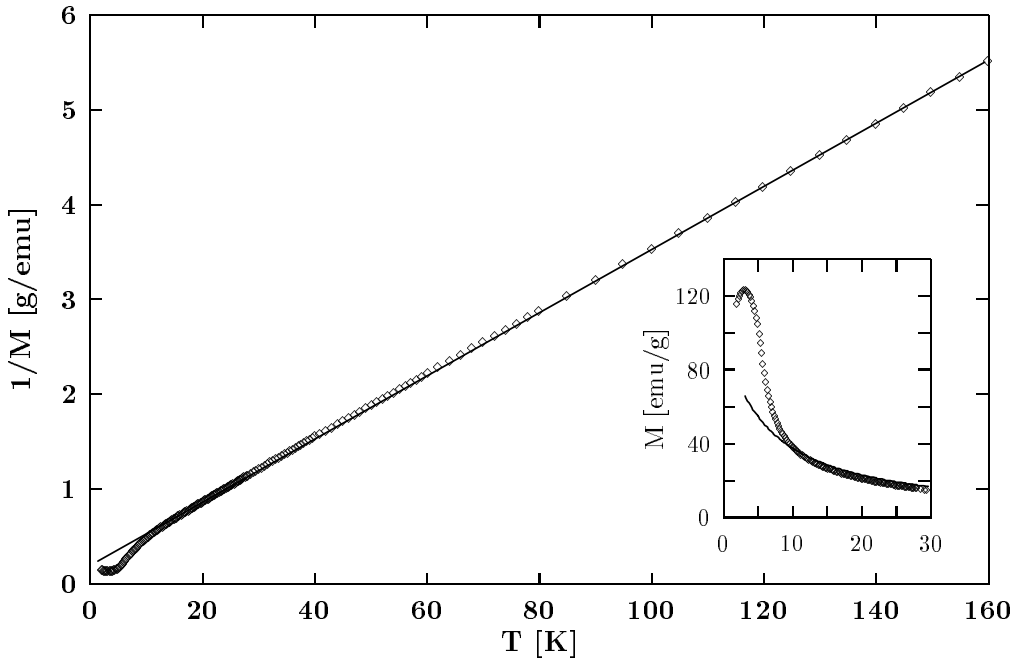

Figure 5.2: Temperature dependence of the inverse magnetization of "Gd_3ReO_8".

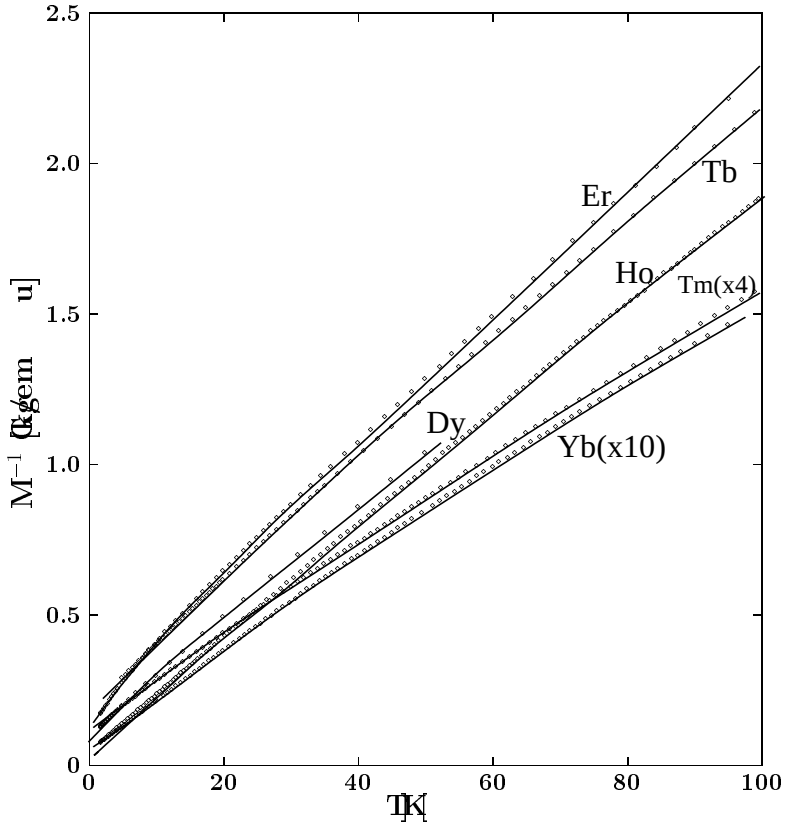

Figure 5.3: Temperature dependence of the inverse magnetization for most of the "Ln_3ReO_8" compounds. For clarity the curves of the Tm- and the Yb-samples have been multiplied by the indicated factors.

"Dy_3ReO_8" had been chosen for further experiments due to its easy preparation leading to pure products. But various syntheses with Dy_2O_3 and ReO_2 in ratio 1 : 2 in sealed Pt/Rh (90/10)-tubes and at temperatures above 1773 K led to products of different optical appearance yielding, nevertheless, very similar powder patterns in good agreement with the cubic $Fm\bar{3}m$ phase. Homogeneous powders with a dark yellow, light to dark brown or black colour trickled out of the opened tubes, even black octahedral shaped crystals with edges up to 100 µm have been obtained twice. Especially these single crystals offered challenging tests for the very unusual coordinations of Ln and Re in the case of a fluorite-type structure.

5.2 Structural details of "Dy_3ReO_8"

As written above the optical appearance of the obtained "Dy_3ReO_8" samples varied significantly, even for virtually the same conditions of syntheses. E.g., two sealed Pt/Rh (90/10)-tubes filled with the same educts and heated simultaneously in the same Al_2O_3-crucible, gave a well crystalline black reaction product in one tube and a fine brown powder in the other. As Dy_3ReO_8 is expected to be white or at least of light colour only, the observed black and brown colours were assigned to oxygen vacancies in different amounts, i.e. $Dy_3ReO_{8-\delta}$. Neutron powder diffraction experiments have been performed for a brown and a black "$Dy_3ReO_{8-\delta}$" sample using ROTAX at ISIS in Didcot, UK, to check this assumption.

One additional data set has been recorded for a silicon standard to determine the present set of instrumental parameters most reliably. Three detector banks at diffraction angles of 30°, 90° and 158° have been used simultaneously, *figure 5.4* shows the diffraction pattern from the black "$Dy_3ReO_{8-\delta}$" sample as seen by the 90° bank and the calculated pattern of the Rietveld refinement using GSAS [67] based on the fluorite-type structure model for "$Dy_3ReO_{8-\delta}$".

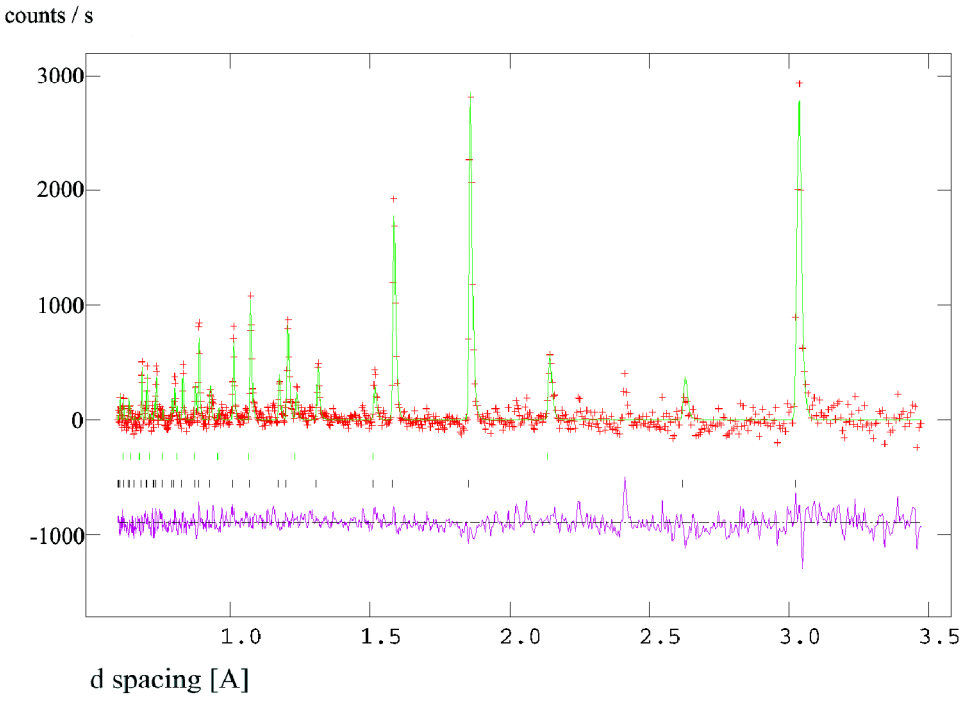

Figure 5.4: Neutron diffraction pattern of "$Dy_3ReO_{8-\delta}$" including observed (red) and calculated (green) pattern, difference plot (blue) and reflection markers (green: vanadium sample holder, black: structure model cubic $Fm\bar{3}m$ phase)

Due to the small amount of sample and the high absorption coefficient for thermal neutrons of Dy, the intensities are too low to establish a precise structure model, but an additional reflection is clearly observed at about 2.412 Å, not explained by the cubic face-centred fluorite-type structure. An additional reflection is also observed for the brown "$Dy_3ReO_{8-\delta}$" sample, but at 2.332 Å and with only about half the relative intensity as compared to the black sample.

These additional reflections were the first indications of a superstructure, especially for the oxygen sublattice which deviates from the fluorite-type. The contribution from the oxygen ions to the X-ray structure factors is too small, so that this additional reflection was not observed in the laboratory X-ray pattern. Based on these hints for a superstructure, high-resolution synchrotron powder diffraction patterns have been recorded in transmission geometry from flat samples of the black and brown "$Dy_3ReO_{8-\delta}$" specimens, respectively.
The patterns revealed both, a splitting of the strong reflections and additional weak superstructure peaks. In the next step of approaching the correct structure of "Dy_3ReO_8" the diffraction pattern was indexed, based on a monoclinic unit cell a_{mon} = 6.4215(3) Å, b_{mon}= 7.4429(1) Å, c_{mon} = 6.4176(2) Å and β_{mon} = 109.371(2)°. The most pronounced effects of splitting and superstructure could be explained, and a structure model was derived in space group $P2_1/m$ with the cation sites split into one Re and three Dy sites, see *table 5.2*. The relationship to the fluorite unit cell, $\{a_{kub},b_{kub},c_{kub}\}$, is given by:

$$a_{mon} \sim 1/2\ (a_{kub} - c_{kub}) + b_{kub},$$
$$b_{mon} \sim a_{kub} + c_{kub},$$
$$c_{mon} \sim 1/2\ (a_{kub} - c_{kub}) - b_{kub},$$
$$\cos \beta_{mon} \sim -1/3.$$

However, this model does still not describe the correct crystal structure of "Dy_3ReO_8", although a considerable improvement is achieved compared to the proposed fluorite-type structure. Some features of the high-resolution diffraction pattern are still not explained and a reliable localization of the oxygens is not possible. Therefore, electron diffraction in a transmission electron microscope was applied to clarify the correct unit cell and symmetries, see *figures 5.5* and *5.6*.

Space group	$P2_1/m$
Atom sites	Re (½, 0, ½)
	Dy(1) (0, 0, 0)
	Dy(2), Dy(3) (x, ¼, z)
Lattice constants	a = 6.4215(3) Å b = 7.4429(1) Å c = 6.4176(2) Å
β	109.371(2) °

Table 5.2: Structure parameters of a "Dy_3ReO_8" superstructure model.

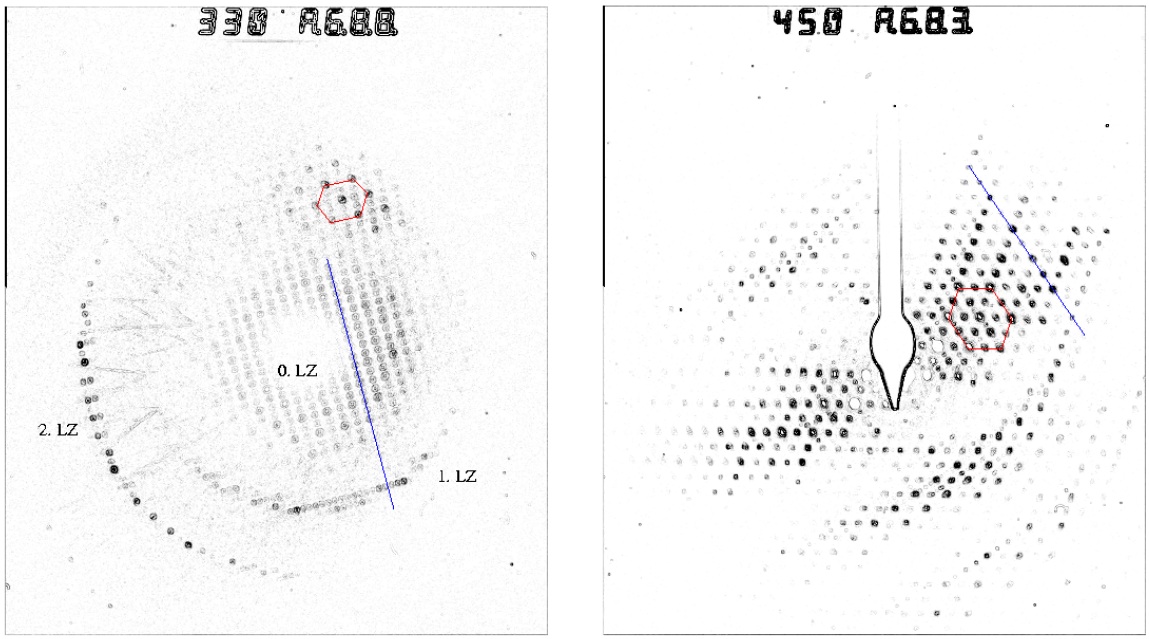

Figures 5.5 and 5.6: Electron diffraction patterns along the zone axes [010] (left) and [100] (right).

Accordingly, a C-centred orthorhombic structure is found with a = 14.8448(1) Å, b = 14.8878(2) Å and c = 10.4782(1) Å, obtained from a profile matching based on the synchrotron diffraction data, see *figure 5.7*. Furthermore, a c-glide plane perpendicular to the a- or b-axis is confirmed by the extinction rules, observed in electron diffraction. The space group Ccmb in non-standard setting was used for profile matching.

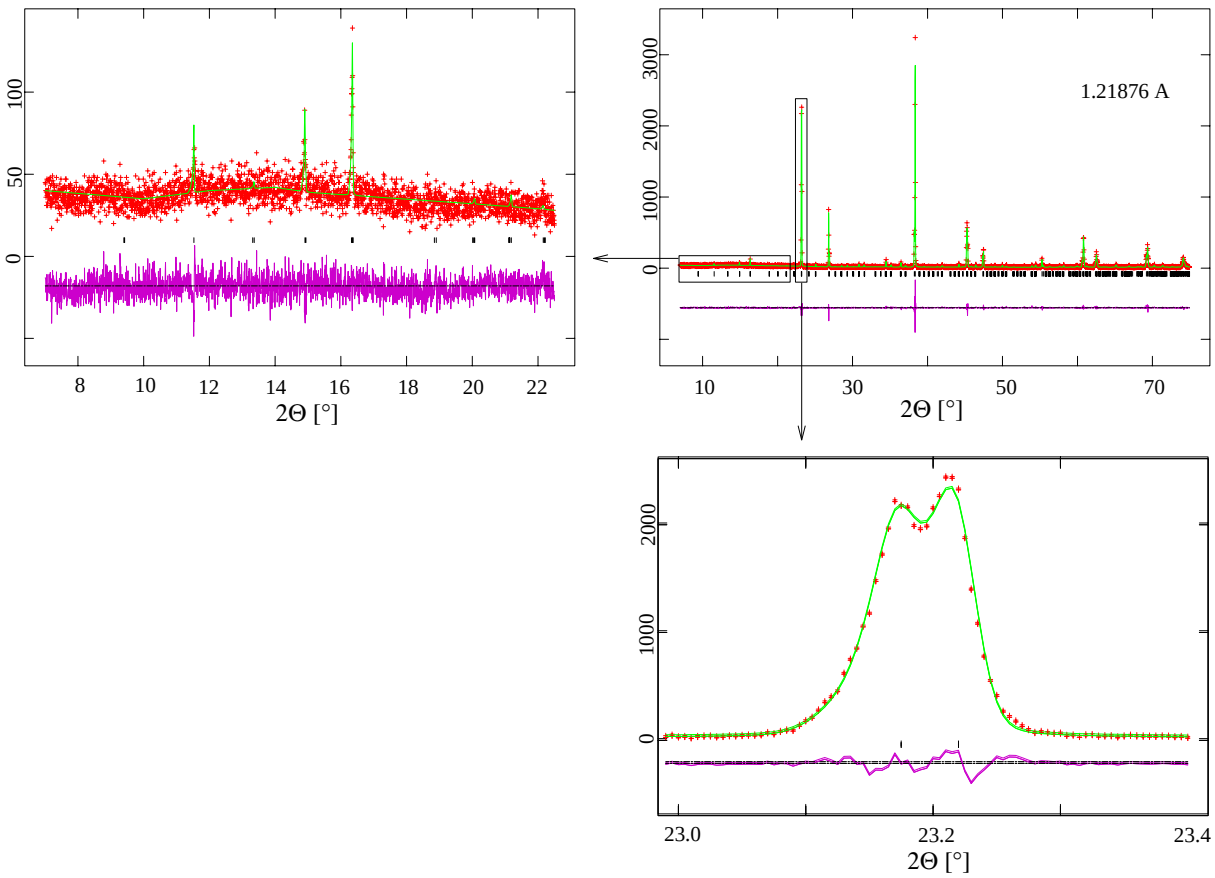

Figure 5.7: Observed and calculated high-resolution diffraction pattern for the black “Dy_3ReO_8” sample. The calculated pattern is the result of a profile matching, based on the C-centred orthorhombic unit cell found in electron diffraction.

Single crystal diffraction data have been collected from 11 different crystals, using an Xcalibur diffractometer with CCD detector from Oxford Instruments and the image-plate system IPDS II from STOE. All reflections with at least 1‰ of the intensity of the strongest reflections could be indexed, based on a smaller pseudo-cubic unit cell $\{a_{pc},b_{pc},c_{pc}\}$ with

$$a_{pc} = 1/2\ (a - b)\ ,$$
$$b_{pc} = 1/2\ (a + b)\ ,$$
$$c_{pc} = c\ .$$

Only a few very weak reflections could be detected with indices (h/2,k/2,l), indicating a larger unit cell in agreement with electron diffraction. Internal R-values between 6.8% and about 11% have been determined for orthorhombic symmetry, and reliable cation positions could be found in space groups Ccmb and Ccmm by direct methods or via Patterson function. Both the extinction rules and the observed intensities require a twinning according to $a_2 = b_1$, $b_2 = a_1$, $c_2 = c_1$ with domain fractions of (or at least very close to) exactly 50%. The cation sublattice is very similar to that of a fluorite-type structure as expected from the similarities in the diffraction patterns. Unfortunately, no reliable refinement of oxygen positions was successful, although very promising start models could be established by difference Fourier analyses. The detailed crystal structure of "Dy_3ReO_8" is still an open challenge for structure determination, but nevertheless, the proposed and unreasonable fluorite-type structure for this compound is clearly disproved and strong evidence for a superstructure cell is presented.

5.3 Structural details of new Y-Re-Oxides

In 1981 Baud et al. reported on the monoclinic Y_3ReO_8, space group $P2_1/a$, and its relationship to the cubic Y_3ReO_8 crystallizing in the fluorite structure [29]. The unit cell of the monoclinic compound with a = 14.391(10) Å, b = 7.196(5) Å and c = 6.045(5)Å and its monoclinic angle β = 112.08(5)° has one Re, three Y and eight O-sites (4e). Having been prepared at 1173 K this phase has been titled as a high temperature phase.

When prepared similar to the $Ln_5Re_2O_{12}$ (Chapter 4) from Y_2O_3 and ReO_2 in ratio 1 : 1 a grey powder appeared from the Pt/Rh-tube after annealing for 24 h at 1773 K. Under the light microscope small octahedral shaped crystals became visible and have been isolated for single crystal diffraction. The grey powder has been investigated using laboratory and synchrotron powder diffractometry. The results of these experiments are summarized in the coming two sections.

5.3.1 $Y_7ReO_{14-\delta}$

One of the octahedral shaped single crystals of the yttrium rhenium oxide with an edge length of approximately 80 µm has been selected for a single crystal structure analysis using an Oxford Diffraction Xcalibur diffractometer in κ-geometry using a CCD detector. 560 reflections, from which 128 are unique, have been collected using molybdenum Kα radiation, wavelength 0.7103 Å. The software packages SHELXS and SHELXL [58, 59] have been used for structure solution and refinement, respectively, as included in X-STEP32 [68].

The refinement using a cubic cell, space group $Fm\bar{3}m$, as structure model led to R values of R_1 = 4.20% and wR_2 = 8.56% for all reflections with $I > 2\sigma$. The composition revealed $Y_7ReO_{14-\delta}$, the lattice constant a = 10.4770 Å [69]. The details of the structure determination of $Y_7ReO_{14-\delta}$ are summarized in *Table 5.3*.

Empirical formula	$Y_7ReO_{14-\delta}$
Formula weight	1032.54 g/mol
Crystal shape and size	Octahedron, 80 µm edge length
Temperature during measurement	299(1) K
Wavelength	0.7103 Å (Mo Kα)
Space group	$Fm\bar{3}m$
Unit cell dimensions	a = 10.4770(14) Å, V = 1150.0(3) $Å^3$
Calculated density	ρ_{cal} = 5.964 g/cm^3
Formula units per unit cell	Z = 4
Absorption coefficient	45.444 mm^{-1}
F(000)	1840
θ range for data collection	3.37 – 30.17°
Limiting indices	$-14 \le h \le 11$, $-8 \le k \le 12$, $-10 \le l \le 15$
Reflections collected / unique	560 / 128, R_{int} = 5.63%
Completeness	94.8%
Refinement method	Full matrix least-squares on F^2
Data / restraints / parameters	128 / 0 / 14
GOF on F^2	1.126
Final R indices ($I > 2\sigma$)	R_1 = 4.20 %, wR_2 = 8.56 %
Extinction coefficient	0.00056 (10)

Table 5.3: Details of the experimental conditions for the structure determination of $Y_7ReO_{14-\delta}$.

The atomic parameters are given in *Table 5.4*, the bond lengths in *Table 5.5*.

Atom	Site	x/a	y/b	z/c	Occupation
Re	(4b)	½	½	½	1.00
Y(1)	(4a)	0	0	0	1.00
Y(2)	(24d)	0	¼	¼	1.00
O(1)	(32f)	0.1332(9)	0.1332(9)	0.1332(9)	1.00
O(2)	32(f)	0.6058(11)	0.6058(11)	0.6058(11)	0.77(8)

Table 5.4: Atomic parameters of $Y_7ReO_{14-\delta}$.

Pair	Bond length [Å]
Re – O(2)	1.92(2)
Y(1) – O(1)	2.417(17)
Y(2) – O(1)	2.223(5)
Y(2) – O(2)	2.407(9)

Table 5.5: Selected bond lengths in $Y_7ReO_{14-\delta}$.

The crystal structure of $Y_7ReO_{14-\delta}$ is closely related to the fluorite type. As a result of the ordered distribution of the metal ions, the lattice constant is doubled, the cell 8-folded. Also the oxygen sites prove the relation to the fluorite structure. The oxygen positions are near to (1/8, 1/8, 1/8) and (5/8, 5/8, 5/8).

With only 77(8)% of the O(2)-site occupied, the site occupation factor is in good agreement with the stoichiometry $Y_7ReO_{14-\delta}$ having a theoretical site occupation factor of 75% and rhenium in its highest oxidation state of (+7). *Figure 5.8* represents the crystal structure of $Y_7ReO_{14-\delta}$.

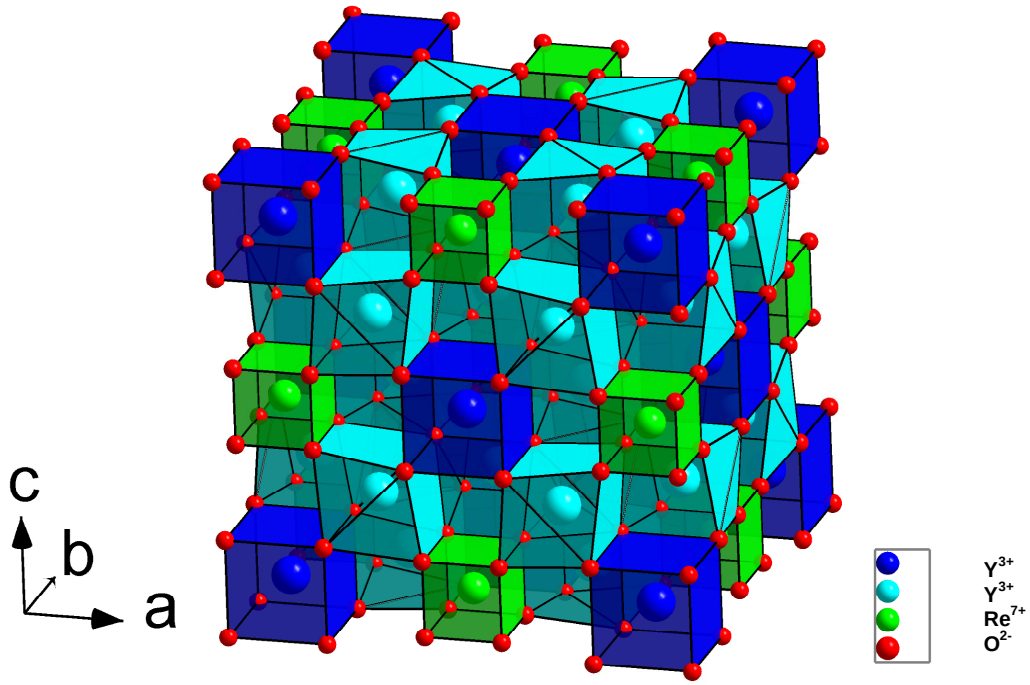

Figure 5.8: Crystal structure of $Y_7ReO_{14-\delta}$.

A small amount of $Y_7ReO_{14-\delta}$ -crystals had been annealed at 973 K, yielding still the same crystal structure afterwards. This is another prove of the rhenium oxidation state +7, since any other compound with rhenium in a lower oxidation state is expected to oxidize to Re(+7) under such conditions.

For the evaluation of the magnetic measurements on $Y_7ReO_{14-\delta}$ the Curie-Weiss law had been modified by a temperature independent contribution M_0 leading to:

$$M(T) = \frac{C}{T-\theta} + M_0$$

The temperature dependence of the magnetization has been measured and fitted with the modified Curie-Weiss law yielding $M_0 = 4.24 \cdot 10^{-5}$ emu, $\theta = -4$ K and a magnetic moment of 0.6 μ_B per formula unit $Y_7ReO_{14-\delta}$. The measured data and the resulting curve for 11.75 mg sample material are shown in *figure 5.9*.

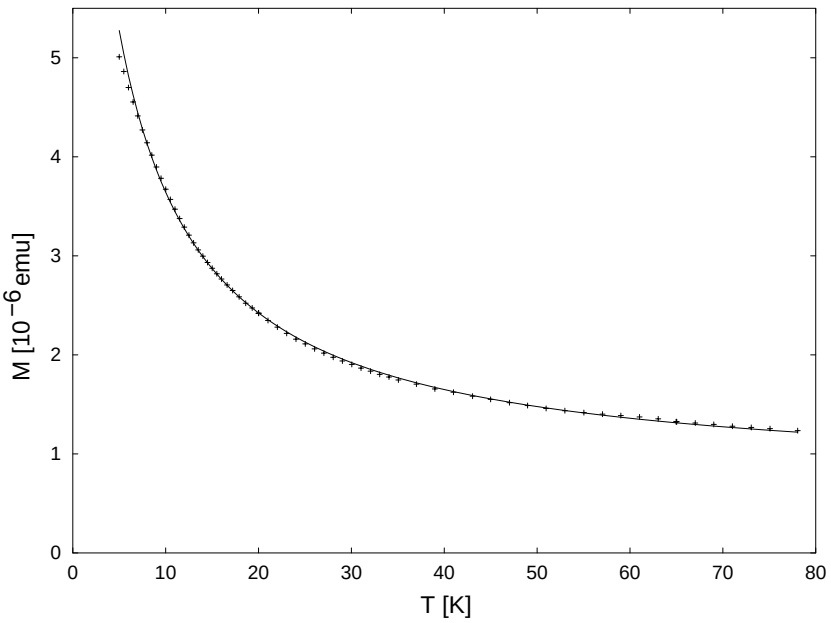

Figure 5.9: Temperature dependence of the magnetization of 11.75 mg $Y_7ReO_{14-\delta}$

Some other octahedral shaped crystals from the same reaction show, though very weak, additional reflections breaking up the conditions for F-centering. These reflections indicate a more complicated structure with deviations from a random distribution of the O(2)-site vacancies.

The crushed material revealed several types of derivatives from the fluorite type by electron diffraction. The pattern of some of these separated crystals can be indexed based on an A-centered orthorhombic cell $\sqrt{2}\ a_F$ x $\sqrt{2}\ a_F$ x $2a_F$ yielding a 4-fold fluorite superstructure cell.

5.3.2 $Y_{3-x}Re_{1+x}O_8$

Prepared by the sealed tube method with Y_2O_3 and ReO_2 in ratio 1 : 1 the product appeared as a light grey powder. A powder pattern from this compound taken in the laboratory gave an indication for a new rhombohedral structure but better resolution was required.

Therefore a pattern had been taken at the beamline B2 at DESY / HASYLAB, Hamburg using a wavelength of 1.2006 Å. The reflections could be indexed easily in a primitive rhombohedral cell with lattice constants a = 7.37941(19) Å and c = 9.38011(21) Å.

X-ray fluorescence analysis yielded the stoichiometry $Y_{2.9}Re_{1.1}O_8$. Rietveld refinement using a fluorite-related structure model, space group $P\bar{3}m$ and Re- and Y-ions sharing their four sites statistically, led to a good correspondence of observed and calculated pattern. Only the (010) reflection is shifted to a slightly higher, the (101) and (102) reflections are shifted to a slightly lower 2θ angle. *Figures 5.10* and *5.11* present this pattern taken from synchrotron data. The calculated pattern, reflection markers and difference plot are also displayed. The 2θ angles from 10° to 22° have been magnified for a better view on the shifted reflections.
Table 5.6 summarizes the crystallographic data of the new yttrium rhenium oxide.

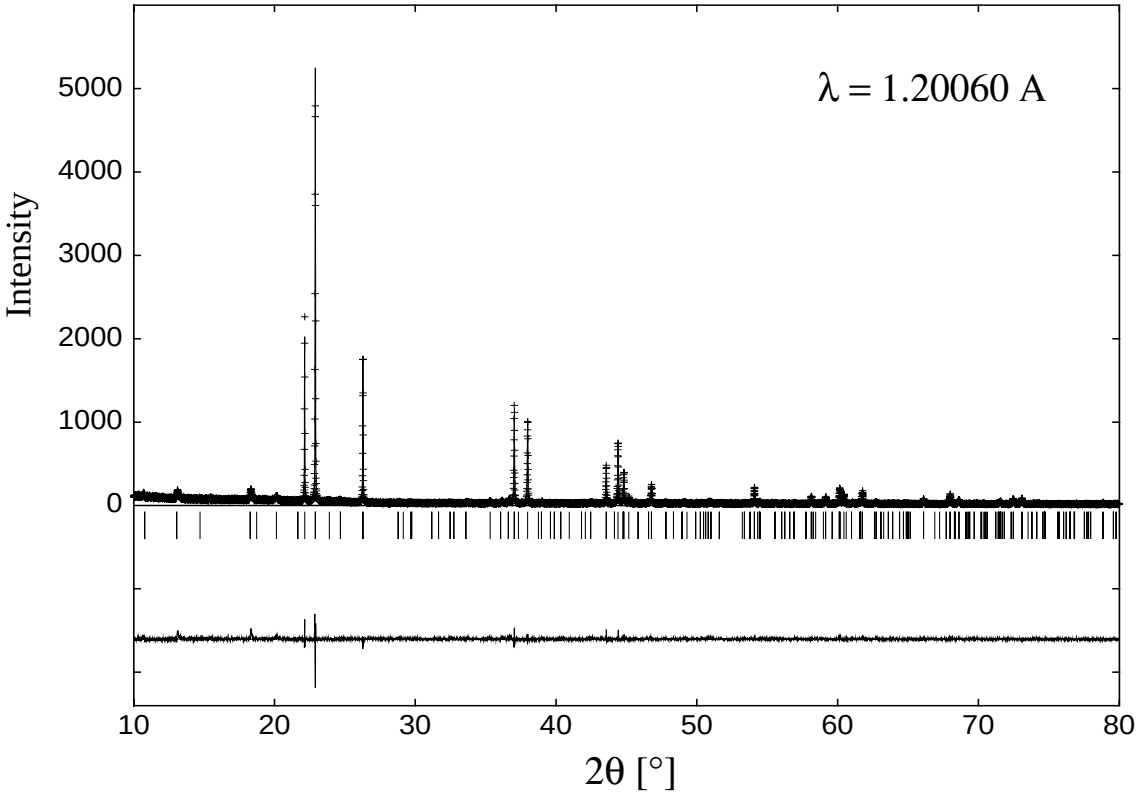

Figure 5.10: Observed and calculated pattern of $Y_{2.9}Re_{1.1}O_8$.

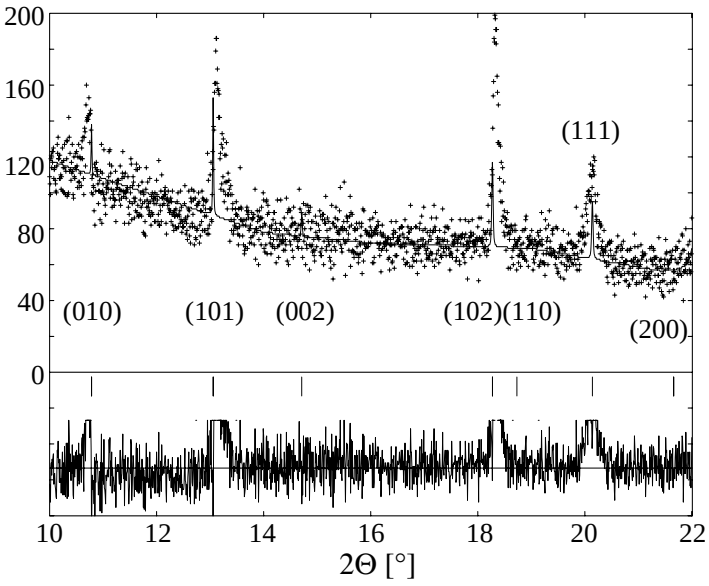

Figure 5.11: Observed and calculated pattern of $Y_{2.9}Re_{1.1}O_8$. The 2θ angles from 10° to 22° have been magnified for a better view on the shifted reflections.

Composition	$Y_{2.9}Re_{1.1}O_8$			
Space group	$P\bar{3}m$			
Lattice constants	a = 7.37941(19) Å b = 9.38011(21) Å			
Atom positions	Atom	x/a	y/b	z/c
	Y(1), Re(1)	0	0	0
	Y(2), Re(2)	1/3	2/3	0.684(1)
	Y(3), Re(3)	1/2	0	0
	Y(4), Re(4)	0.382(1)	0.164(1)	0.6769(8)
	O(1)	0	0	0.27(1)
	O(2)	1/3	2/3	0.90(1)
	O(3)	1/3	2/3	0.43(1)
	O(4)	0.514(9)	0.028(9)	0.225(7)
	O(5)	0.819(7)	0.637(7)	0.921(6)
	O(6)	0.871(8)	0.742(8)	0.391(5)

Table 5.6: Crystallographic data for $Y_{2.9}Re_{1.1}O_8$.

For a better understanding of the shifted reflections high resolution transmission electron micrographs have been taken from a small amount of $Y_{2.9}Re_{1.1}O_8$. Electron diffraction images (*figure 5.12*) yielded reflection splitting and diffuse phenomena. While the fluorite related [220]-planes (d = 1.845 Å) are normally arranged, fluctuations appear in the sequence of the [100]-planes yielding a d value with a small deviation from $d(220)\cdot\sqrt{12} = a_0\cdot\sin 60°$.

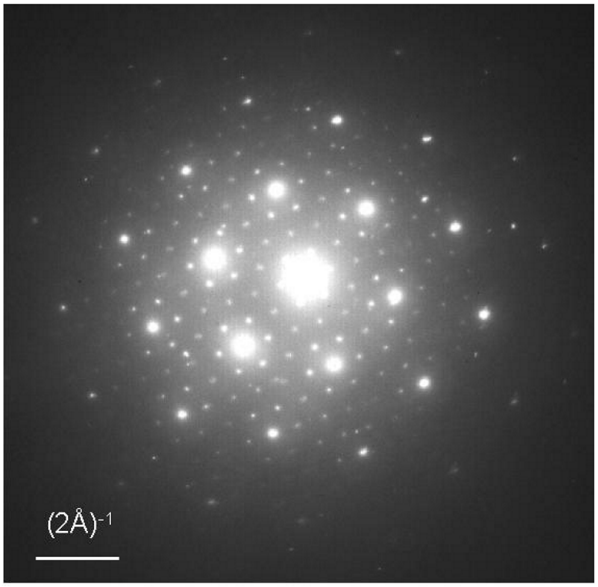

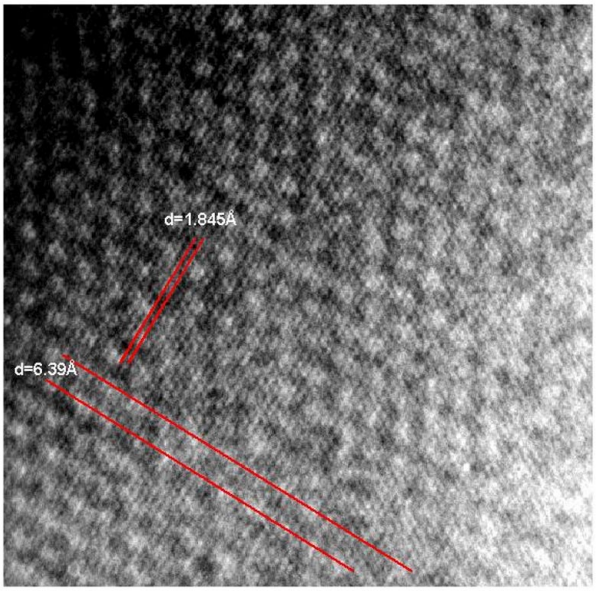

Figure 5.12: Electron diffraction pattern of the [001]-plane and HRTEM image of $Y_{2.9}Re_{1.1}O_8$.

5.4 Electrical resistivity of the "Ln_3ReO_8"

Gold wires of 10 µm diameter have been attached to opposite faces of octahedral shaped crystals of "Ln_3ReO_8" with Ln = Eu, Dy and Y with edge lengths of 50, 80 and 100 µm, respectively. The silver paste contacts had been annealed for 5 min in air at 460°C without any change in the appearance of the crystals. The electrical resistivity has been determined as a function of temperature by the two point method, i.e. the corresponding voltage for a specific current flow was measured at the gold wires close to the crystal faces. All samples appeared as semi conductors with band gaps of 192.2 meV for "Eu_3ReO_8", 159.7 meV for "Dy_3ReO_8" and 157.4 meV for "Y_3ReO_8". *Figure 5.13* illustrates the logarithmic resistivity versus the inverse temperature.

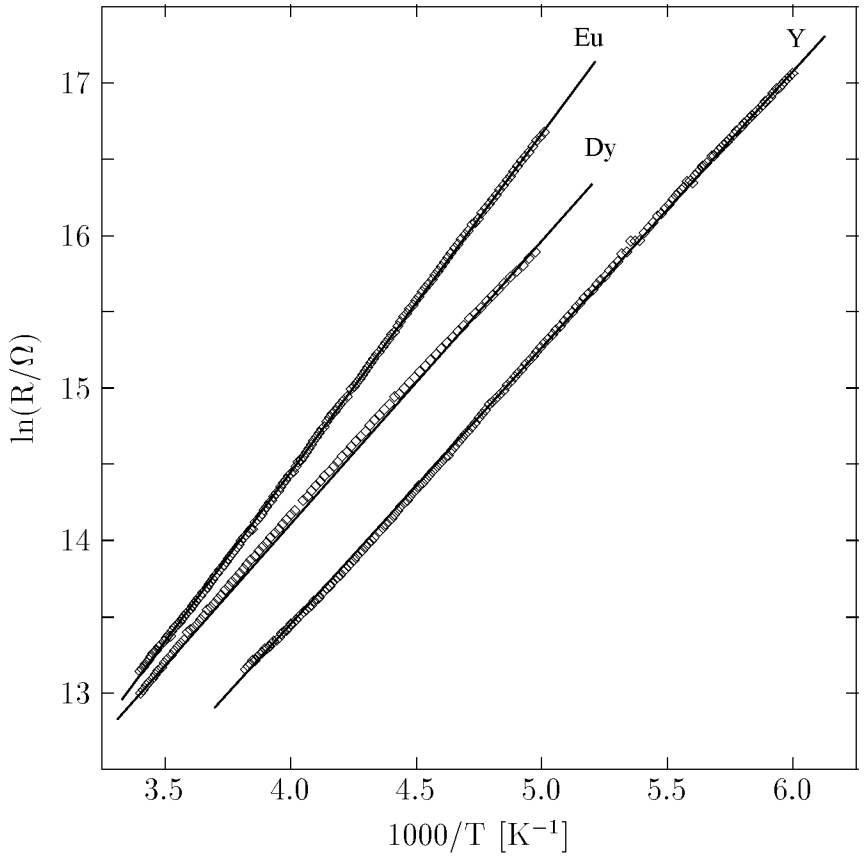

Figure 5.13: Logarithmic resistivity versus inverse temperature of "Ln_3ReO_8" single crystals with Ln = Eu, Dy and Y from left to right.

The crystal structure determination of "Ln_3ReO_8" phases is a very difficult task due to complicated superstructures and twinning. The cation sublattice is very similar to that of a fluorite-type structure, and the oxygen positions cannot be resolved because of the low scattering power for X-rays. A qualitative step further is therefore expected from neutron single crystal diffraction or good resolution neutron powder diffraction with high counting statistics. However, neutron diffraction requires large amounts of sample, which is not only a financial concern, but also a question of homogeneity. Both single crystal X-ray and electron diffraction gave evidence for different degrees of symmetry reduction in the superstructures. Probably a whole set of crystal structures (co-)exist with only slight differences. Furthermore, some kind of healing process accompanied by crystal growth takes place while storing the crystals at room temperature.

6 A new binary rhenium oxide: Re_3O_{10}

Regarding the edges of the diagram of known phases in the system $Ln_2O_3 – ReO_2 – Re_2O_7$ the still missing structure solution of Rhenium(V)oxide appears immediately.
Literature gives the only hints of Re_2O_5 as a blackish blue product yielding a tetragonal structure with lattice constants a = 5.80(3) Å and c = 12.87(3) Å [21] or having an orthorhombic unit cell related to the cubic ReO_3 with $b \approx c \approx a_c \approx 3.747$ Å and $a \approx 2\ a_c\sqrt{2} \approx 10.598$ Å [22].
Encouraged by a straight forward preparation of Ti_2O_3 from a stoichiometric 1:1 mixture of TiO and TiO_2 with an arcmelter the idea appeared to produce Re_2O_5 the same way from Rhenium(IV)- and Rhenium(VI)oxide [70].

6.1 Preparation

As a first attempt a mixture of ReO_2 and ReO_3 in ratio 1:1 was ground under acetone in an agate mortar and formed to pellets under a pressure of 10 tons. These metallic-purple coloured pellets have been heated in an arc melter (BÜHLER Lichtbogenanlage AM) under argon atmosphere for about 10s in turns yielding a blue compound on the water cooled copper ground plate of the arc melter and a certain amount of a gaseous phase in the furnace. After opening the reaction chamber the blue powder became black and wet within a few seconds.
To protect the reaction product from moisture the whole furnace was operated under argon atmosphere in a glove bag for the next run. Hereby, the sample could be collected from the ground plate of the furnace and stored under argon atmosphere. A small amount of a metallic material had been gathered, too. The gaseous phase solidified on the mantle of the arc melter to a dirty white and slightly hygroscopic powder seeming to be Re_2O_7. Later attempts failed again due to moist argon and the inability to extract this moisture by leading the gas through P_2O_5 or H_2SO_4 before entering the reaction chamber.
Based on colour and decomposition behaviour, the product was assumed to be Re_2O_5. For structure determination the material was filled in a 0.5 mm glass capillary and investigated by X-ray powder diffraction using a STOE STADI P diffractometer in Debye-Scherrer mode.

6.2 Structure Analysis

The powder pattern taken directly after the synthesis is shown in *figure 6.1* giving the impression of a rather amorphous material. Only the reflections of metallic rhenium could be identified.

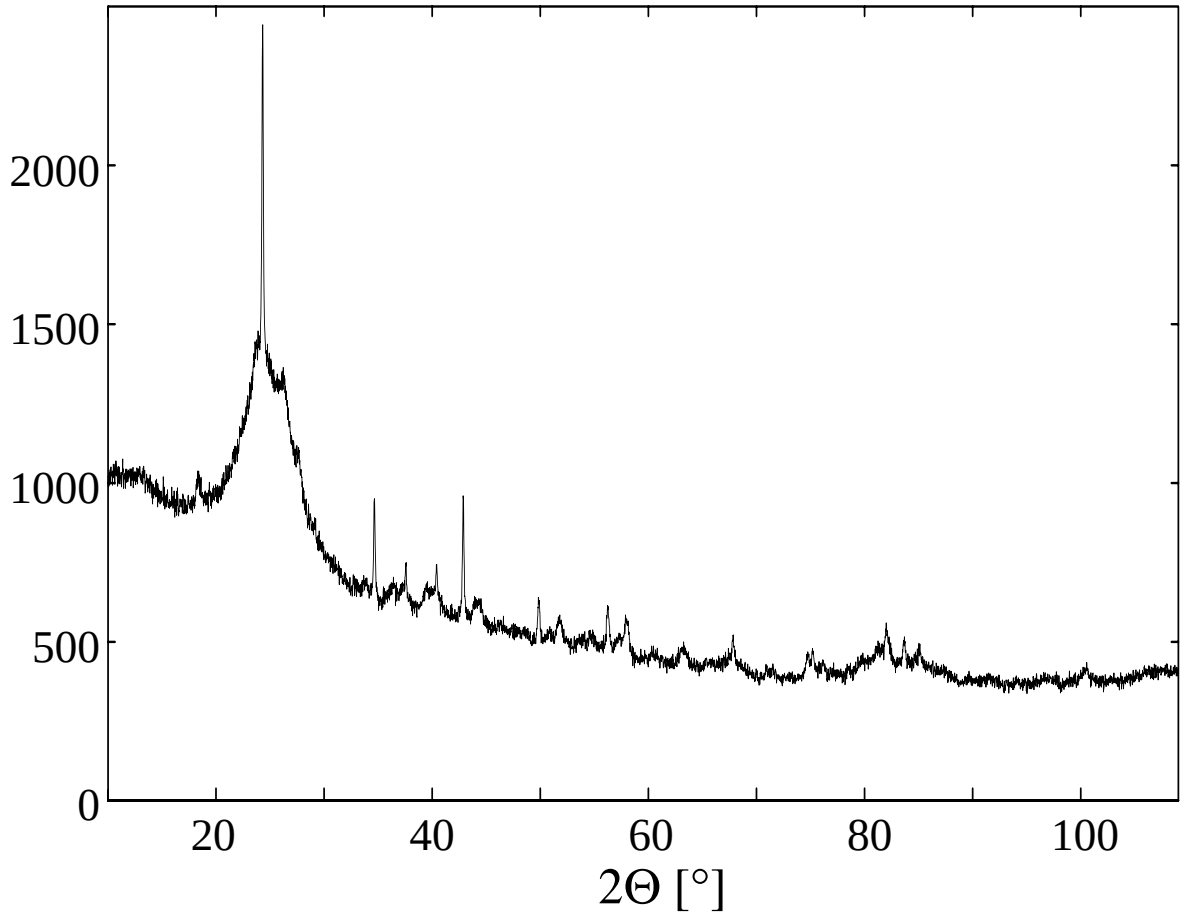

Figure 6.1: X-ray powder pattern of the as prepared sample

Ten weeks later the sample's blue colour in the capillary has been intensified remarkably. After a second measurement the obtained powder pattern indicates a striking change (*figure 6.2*). Nearly all reflections could be indexed with the STOE indexing routine based on a tetragonal cell with a = 5.2 Å and c = 13.3 Å. The (00l)-reflections are extremely broadened. The lattice constants are close to those determined by Tribalat et al. [21], supporting the assumption that Re_2O_5 has been prepared. Therefore it was tried to solve the crystal structure by direct methods from powder data and hereby confirming the proposed stoichiometry.

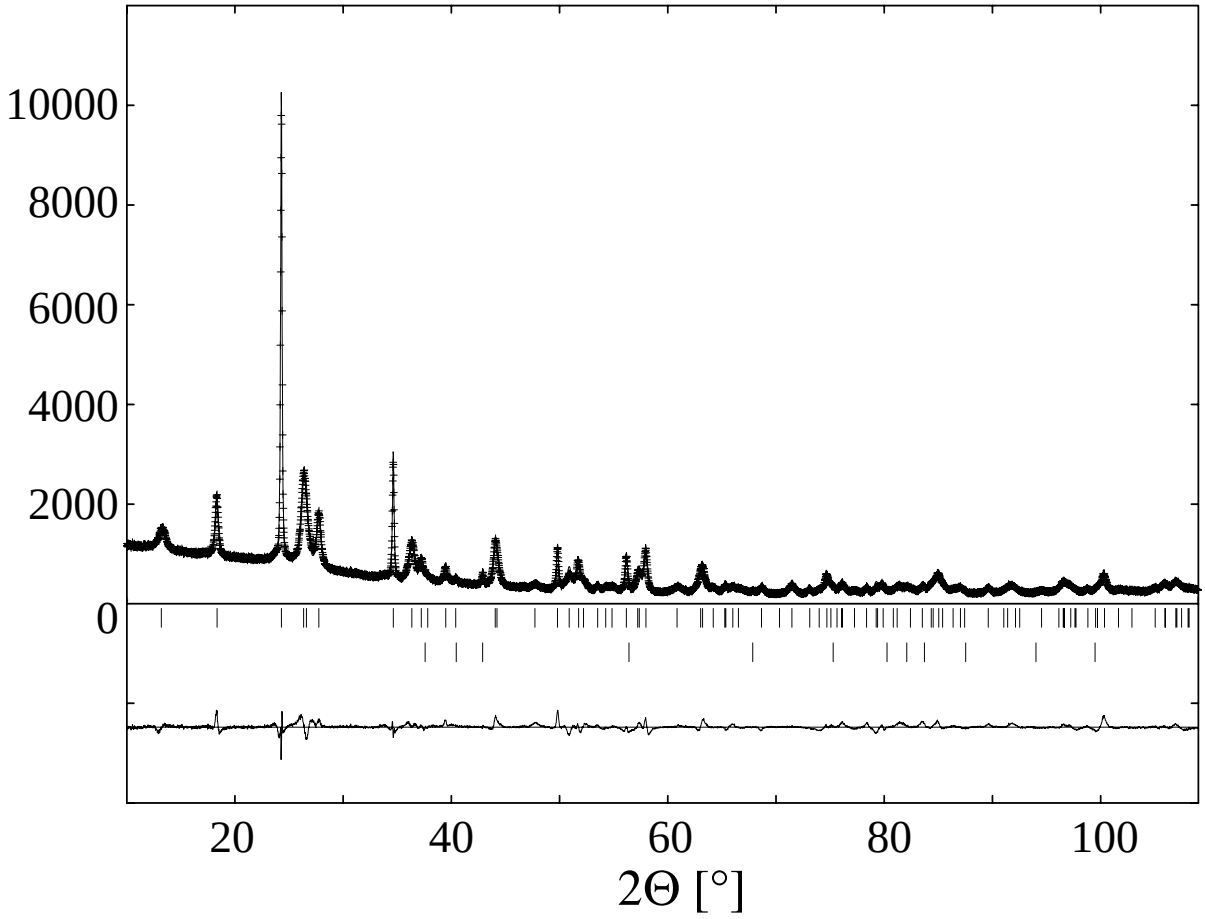

Figure 6.2 Observed and calculated profiles for Re_3O_{10} and difference plot after 10 weeks of annealing. The lower line of reflection marks belongs to metallic rhenium.

No extinction rules in addition to body centering were present. The relative intensities of the (00l)-reflections indicate a $\bar{4}$ axis most probable and thus only the three space groups $I\bar{4}$ (No. 82), $I\bar{4}m2$ (No. 119) and $I\bar{4}2m$ (No. 121) were retained.

In order to deduce the atomic positions additional considerations were necessary. With the volume of the unit cell of around 360 $Å^3$ the volumes per atom for all possible stoichiometries Re_xO_y (x = 2 – 5) were calculated. The density of the new compound had to be lower than the one of ReO_3 and therefore the volume per atom higher than in ReO_3 (13 $Å^3$ / atom). Additionally, the number of atoms should be lower than N = 28. Odd formula units Z are excluded by the supposed tetragonal symmetry, at least two rhenium sites are necessary. All possible compositions are shown in *table 6.1*.

Oxides	Cell volume ($Å^3$)	ρ (g/cm^3)	Volume per oxygen ($Å^3$)
Re_2O_7	1035.5	6.21	18.5
ReO_3	52.7	7.39	17.6
ReO_3 (9 Gpa)	91.2	8.53	15.2
Re_2O_5	432.9	6.94	21.6
α ReO_2	124.9	11.61	15.6
β ReO_2	128.4	11.29	16.1
$Re_6O_{18} \equiv 6ReO_3$	357.6	6.53	19.9
$Re_8O_{20} \equiv 4Re_2O_5$	357.6	8.41	17.9
$Re_6O_{20} \equiv 2Re_3O_{10}$	357.6	6.68	17.9
Re_7O_{22}	357.6	7.69	16.3

Table 6.1: Cell volume, density and volume per oxygen atom of all mathematical possible binary rhenium oxides.

Although close to the values postulated for Re_2O_5 [21-23], the cell parameters for the unknown oxide Re_xO_y are sufficiently different resulting in a cell volume V of 357.6 $Å^3$ which is much smaller than the cell volume of Re_2O_5 (above 433 $Å^3$). Therfore, before starting a hypothesis about possible sites for Re and O atoms, a reasonable stoichiometry had to be established via the classical volume of oxygen atoms in oxides (~16-17 $Å^3$), the corresponding volumic mass ρ and by comparison with known rhenium oxides. This information is summarized in *table 6.1*. The oxygen number y has to be even (space group symmetry) and should be either y = 18, y = 20 or y = 22 which gives a reasonable volume per oxygen (V/O), i.e. 19.9 $Å^3$, 17.9 $Å^3$ and 16.3 $Å^3$. The first solution leads to the Re_6O_{18} formula which could be a polymorph of ReO_3; taking into account that ReO_3 is already a rather open structure, it seems unreasonable, in a first attempt, to have such a large V/O and correlatively such a low ρ value (and that the powder's colour is deep blue).

The last y value resulting in Re_7O_{22} corresponds to a mixed valence oxide $Re_2^{7+}Re_5^{6+}O_{22}$ which yields a value too low for V/O which is not in agreement with the synthesis procedure and the moisture sensitivity. Finally there remained two possibilities:

- Re_8O_{20} which could correspond to the Re_2O_5 oxide but having an extremely high ρ value which could not be expected after such a crude synthesis.
- Re_6O_{20} corresponding to a mixed valence oxide Re_3O_{10} or $Re_2^{7+}Re^{6+}O_{10}$, a formula being reasonable with the colour of the powder, the V/O and ρ values.

The relative intensities of reflections (00l) strongly indicate $\bar{4}$ symmetry with two Re-sites Re1 and Re2 at z1 and z2 with corresponding multiplicities m1:m2 = 2:1.

The 8g and 8i-sites were no reasonable positions for rhenium atoms. Since $a_0/\sqrt{2}$ = 3.66 Å is close to Re-Re-distances the 4e site (0,1/2,z) or the equivalent 4f site (0,0,z) with z close to zero are reasonable for the rhenium atom Re1. Therefore a structure with Re1 on the 4f site was chosen as a start model for Rietveld refinements. Because of c = 13.3 Å additional rhenium atoms Re2 had to be placed on the 2d site (0,1/2,1/4). This model gave convergence, the refinements led to z = -0.023 for the Re1 atoms. Any other model with more or less than six rhenium atoms in the unit cell obtained poorer agreement after refinement. However, a significant improvement was achieved by including a disorder of Re2, (2d) (0, ½, ¼) sof =1 → (8h) (x, ½+x, ¼) sof=1/4 with x refined to –0.08.

Based on the Re substructure oxygen positions were successively searched by Difference Fourier Analysis, revealing O1 at (8g) (x, x, 0), x ≈ 0.25 and O2 at (4g) (0, ½, z), z ≈ 0.12. Another oxygen position O3 was found at z ≈ ¼, but appeared to be disordered. The disorder for O2 is only introduced to simulate a huge thermal displacement. Reasonable bond lengths are obtained for Re2, only at the center 2d (0, ½, ¼). The best results of the Rietveld refinement with FULLPROF [61] are summarized in *table 6.2* and observed and calculated profiles are compared in *figure 6.3*. The effect of absorption has been calculated numerically and was taken into account as additional factors to the calculated intensities at each 2θ-point.

6.3 Results

The crystal structure of the mixed valence (VII,VI) rhenium oxide Re_3O_{10} is built up by $[ReO_3]_n$ layers of $[ReO_5]$ corner sharing square pyramids. These layers are linked to each

other by [ReO_6] octahedra, sharing the apical oxygen of the square pyramids and oxygens of the opposite octahedra. The structure is shown in *figure 6.3*, the two alternative coordinations of Re2 with O3 due to the disorder of O3 are displayed in *figure 6.4*. The [ReO_6] octahedra are rather regular, but the Re2-ion is highly disordered.

The highly hygroscopic trirheniumdecaoxide was prepared from ReO_2 and ReO_3 in an arc melting furnace under Ar-atmosphere. The as prepared material appeared rather amorphous, but crystallized during 10 weeks of annealing at room temperature. The composition Re_3O_{10} and its crystal structure were solved from X-ray powder diffraction, and Re_3O_{10} is the first example of five-fold coordinated Re. Lattice parameters, colour and instability in the presence of H_2O are very similar for Re_3O_{10} and Tribalat's Re_2O_5; both oxides are probably mixed valence ones. The crystallographic data are sufficiently different to let us suppose that further investigations are necessary to isolate Re_2O_5 and to settle its crystal structure. However, it is also possible that Tribalat's Re_2O_5 was actually Re_3O_{10} as the composition Re_2O_5 was based on electrochemical methods only.

Composition	Re_3O_{10}
Molecular weight	718.6 g/mol
Space group	$I\bar{4}m2$
Unit cell data	a = 5.171(1) Å c = 13.371(6) Å V = 357.5(3) $Å^3$ ρ_x = 6.68 g/cm^3 Z = 2
Atom sites	Re1 4f 0 ½ -0.023(2) sof =1 Re2 8h -0.082(2) 0.418(2) ¼ sof =1/4 O1 8g 0.293(6) 0.293(6) 0 sof =1 O2 4f 0 ½ 0.115(2) sof =1 O3 16j 0.14(2) 0.15(2) 0.23(3) sof =1/2
Reliability values	χ^2 = 4.01 R_F = 5.88 R_{ex} = 4.25

Table 6.2: Structural details of Re_3O_{10}.

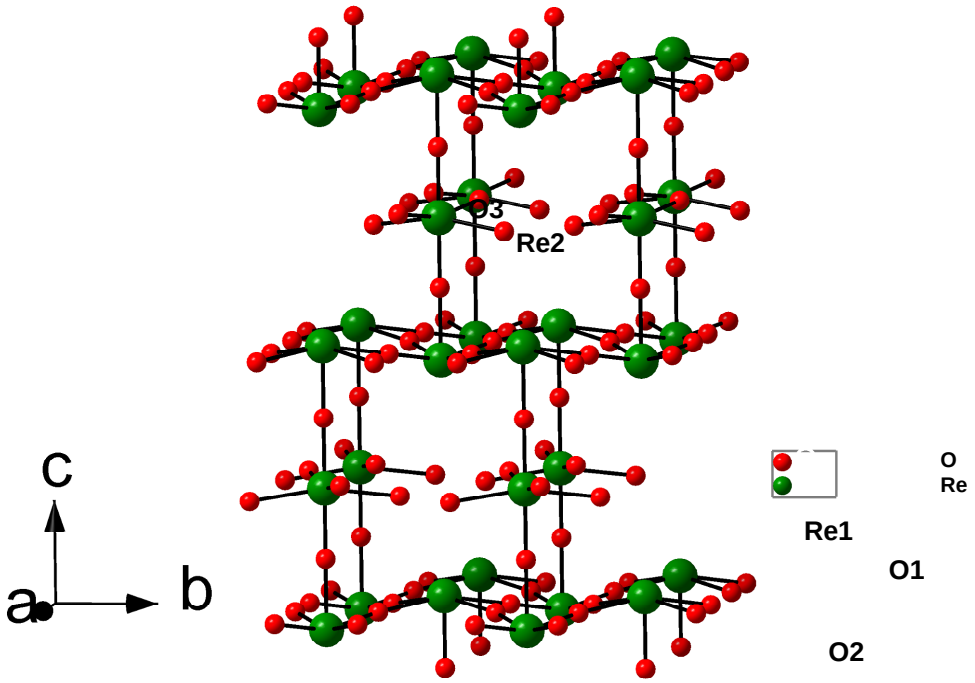

Figure 6.3: The crystal structure of Re_3O_{10}.

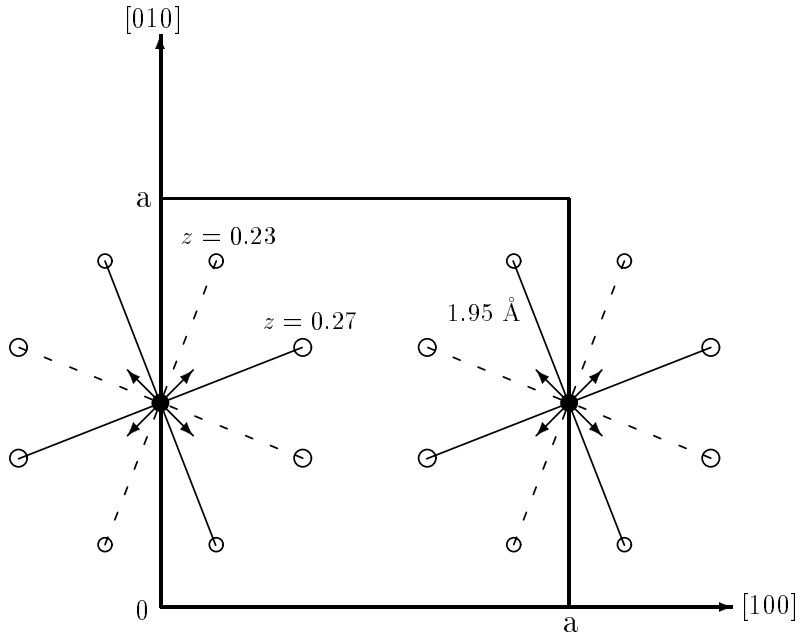

Figure 6.4: View on the ab-plane as z ~ ¼. The two alternative coordinations of Re2 at (0, ½, ¼) and (1, ½, ¼) with O3 are shown as drawn and dashed lines, respectively. The arrows indicate the four disordered positions of Re2

7 Discussion

In this work compounds of different compositions in the system Ln_2O_3 – ReO_2 – ½ $Re2O_7$ (Ln = Y or lanthanide) have been prepared and investigated in respect to their crystal structure and their physical properties as magnetism and conductivity. *Figure 7.1* presents again the scheme of known phases in the system Ln_2O_3 – ReO_2 – ½ Re_2O_7 as *figure 2.1*, but completed by the recently established phases. Blue and yellow circles symbolize the already known rare-earth rhenium oxides with or without structure solution, the red numbers the results of this work.

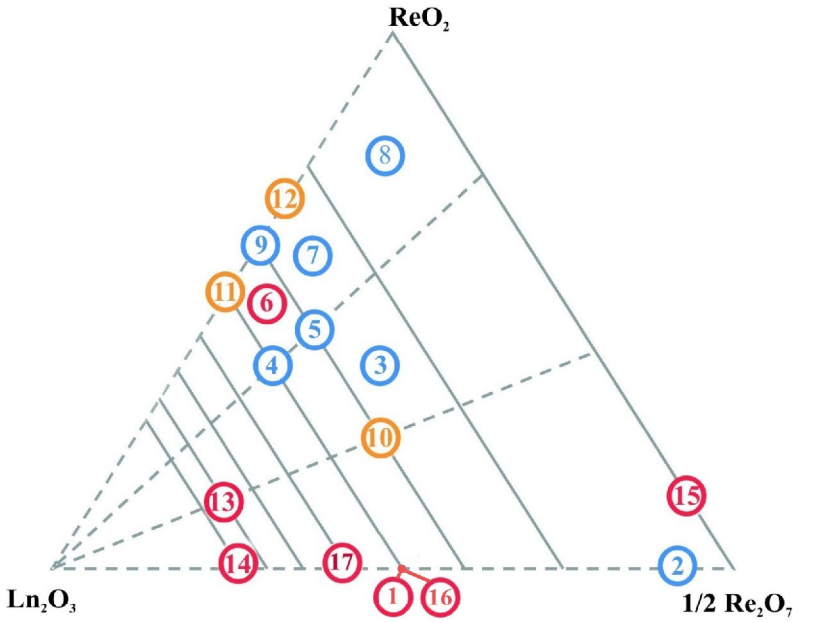

	Ln=
1: Ln_3ReO_8	Y, La-Sm, Gd-Lu
2: $Ln(ReO_4)_3$	Y, La-Lu
3: $Ln_3Re_2O_{10}$	La,Pr
4: Ln_3ReO_7	Nd,Pr,Sm
5: $Ln_4Re_2O_{11}$	Pr-Gd
6: $Ln_5Re_2O_{12}$	Y, Dy, Ho-Lu
7: $Ln_3Re_2O_9$	La,Pr Nd,Sm
8: $Ln_4Re_6O_{19}$	La-Nd
9: Ln_2ReO_5	Y,La,Nd,Sm-Lu
10: Ln_2ReO_6	La
11: $Ln_6Re_2O_{13}$	Nd,Sm,Gd *
12: $Ln_4Re_3O_{12}$	La,Nd*
13: Ln_6ReO_{12}	Ho-Lu
14: Ln_7ReO_{14}	Y
15: Re_3O_{10}	
16: $Ln_{2.9}Re_{1.1}O_8$	Y
17: $(Ln_{0.81}Re_{0.19})_3O_{5.64}$	Gd, Dy, Y

Figure 7.1: Diagram of the system Ln_2O_3 – ReO_2 – ½ Re_2O_7 with the new published Phases (red).

The new ternary compounds have a low Re : Ln ratio with the highest value of 2 : 5 in $Ln_5Re_2O_{12}$.

All syntheses with Re : Ln ratios of 1 :1, 2 :1, or 3 :1 have resulted in rhenium perrhenate hydrates with different water content, even if the samples have been kept in argon atmosphere during all steps, including reaction and opening of the tubes In fact, the influence of argon during all preparation steps in this “sealed tube method” is rather negligible. This has been found first when Tm_6ReO_{12} was re-prepared in air and further supported by the second

preparation of $Ln_5Re_2O_{12}$ when the tubes had not been sealed under argon. Only the success in the preparation of Re_3O_{10} is directly related to the amount of humidity in the argon gas.

During the latter experiments with higher Re : Ln ratios on the educt side not properly sealed tubes led remarkably to well known phases as e.g. $Ln_8Re_4O_{19}$, Ln_6ReO_{12} or $Ln_5Re_2O_{12}$, only. Variation of the reaction temperature from 1073 – 1773 K yielded no improvement. $Ln(ReO_4)_3 \cdot nH_2O$ (Ln = Dy – Lu, n = 1 – 4) appeared in a striking stability.
Therefore, it seems that the sealed tube method has reached its limits for the preparation of new phases in the system Ln_2O_3 – ReO_2 – ½ Re_2O_7, especially rhenium-rich ones. High pressure / high temperature experiments may give an improvement in this case.

Most of the prepared samples contain rhenium in its highest oxidation state +7 with unoccupied 5d- orbitals. Therefore most of the investigated samples showed paramagnetism even at low temperatures. En exception is Yb_6ReO_{12} with an anti-ferromagnetic ordering below T_N = 2.2 K. From the paramagnetic Lu_6ReO_{12} sample the magnetic moment of Re^{+6} had been calculated to 1.5(2) μ_B.
It is more than annoying that both existing capillaries with Re_3O_{10} got irretrievable crashed while being transported to the HASYLAB and its re-preparation failed because of wet argon. The physical properties of a sample crystallizing in such a structure must be very interesting.

Conductivity measurements on single crystals of the formal composition "Ln_3ReO_8" with edge-lenghts between 50 and 100 µm led to the expected semiconducting behaviour with band gaps between 0.19 and 0.15 eV.
The cubic fluorite-type structure for these compounds with Ln^{3+}- and Re^{7+}-ions sharing one site statistically should be ranked as refuted. Still structure solutions of the fluorite related superstructures are lacking. Another point of investigation in this case are the still growing octahedral crystals.
Doubts exist also for the assumed rhombohedral crystal structure of the compounds $(Ln_{0.81}Re_{0.19})_3O_{5.64}$. This preliminary structure model assumes also the Ln^{3+}- and the Re^{7+}-ions statistically situated on one atomic site. The growing of single crystals of at least one of the $(Ln_{0.81}Re_{0.19})_3O_{5.64}$ seems to be necessary for the structure solution.

Taking into account that ternary rhenium oxides e.g. with 3d elements showed interesting physical properties recently the demand for further investigations in the system Ln_2O_3 – ReO_2 – ½ Re_2O_7 with rhenium in an oxidation state <+7 is still given. As an example $Cd_2Re_2O_7$, crystallizing in pyrochlor structure, is a superconductor [71]. Superconductivity has also been postulated for ReO_3 due to its electron– phonon interaction but never confirmed [72].

Another question still to be answered is the confirmation of the high temperature phase of the $Ln_5Re_2O_{12}$. Not only for these samples the necessity for a suitable tube material for high temperature measurements under oxygen excluding conditions and temperatures higher than the re-crystallization point of quartz is still at hand.

Last but not least, a re-preparation of Re_3O_{10} for investigations on its physical properties is of highest interest.

8 References

[1] Noddack, W., Tacke, I. and Berg, O.: *Naturwissenschaften* **13** (1925) 567.

[2] Noddack, I. and Noddack, W.: Sauerstoffverbindungen des Rheniums, *Naturwissenschaften* **17**, (1929) 93-94.

[3] Noddack, I. and Noddack, W.: Die Sauerstoffverbindungen des Rheniums, *Z. anorg. allgem. Chem.* **181** (1929) 1-37.

[4] Peacock, R. D.: Rhenium, *Comprehensive Inorganic Chemistry, Vol 3, Chapter 39* (1973), 905-78.

[5] Rouschias, G.: Recent Advances in the Chemistry of Rhenium, *Chem. Rev.*, **74(5)** (1974) 531-66.

[6] Geilmann, W. and Wrigge, F. W.: Über Rheniumsesquioxyd Re_2O_3, *Z. anorg. allgem. Chem.* **214** (1933) 239-43.

[7] Biltz, W.: Über Rheniumtrioxyd und Rheniumdioxyd, *Z. anorg. allgem. Chem.* **214** (1933) 239-43.

[8] Magneli, A.: Studies on Rhenium Oxides, *Acta Chem. Scan.* **11** (1957) 28-33.

[9] Rogers, D. B., Shannon, R. D., Sleight, A. W. and Gillson, J. L.: Crystal Chemistry of Metal Dioxides with Rutile-Related Structures, *Inorg. Chem.*, **8** (1969) 841-49.

[10] Biltz, W. and Lehrer, G.A.: Rheniumtrioxyd, *Z. anorg. Allgem. Chem.*, **207** (1932) 113-20.

[11] Meisel, K.: Über die Kristallstruktur des Rheniumtrioxids, *Z. anorg. allgem. Chem.* **207** (1932) 121-28.

[12] Sleight, A. W. and Gilson, J. L.: Preparation and Properties of Alkali-Rhenium Bronzes and a WO_3-ReO_3 Solid Solution, *Solid State Communs.* **4** (1966) 601-2.

[13] Dickens, P. G. and Whittingham, M. S.: The Tungsten Bronzes and Related Compounds, *Quart. Rev. Chem. Soc.* **22** (1968) 30-44.

[14] Jørgensen, J.-E., Jorgensen, J. D., Batlogg, B., Remeika, J. P. and Axe, J. D.: Order parameter and critical exponent for the pressure-inducted transitions in ReO_3, *Phys. Rev. B* **33(7)** (1986) 4793-8.

[15] Jørgensen, J. E., Staun Olsen, J. and Gerward, L.: Phase Transitions in ReO_3 Studied by High Pressure X-Ray Diffraction, *J. Appl. Cryst.* **33** (2000) 279-84.

[16] Krebs, B., Müller, A. and Beyer, H. A.: New Type of Oxide Structure: The Crystal Structure of Rhenium(VII)oxide, *Chem. Communs.* (1968) 263-64.

[17] Krebs, B.: Rhenium(VII)oxid und Perrheniumsäure, *Angew. Chem.* **7** (1968) 291.

[18] Krebs, B., Müller, A. and Beyer, H. A.: The Crystal Structure of Rhenium(VII)oxide, *Inorg. Chem.* **8** (1969) 436-43.

[19] Briscoe, H. V. A., Robinson, P. L. and Rudge, A. J.: A New Oxide of Rhenium. Rhenium Pentoxide, *J. Chem. Soc.* (1932) 3087-8.

[20] Roth, W. A. and Becker, G.: Rhenium pentoxide, *Ber.***65 B** (1932) 373.

[21] Tribalat, S. Delafos, D. and Piolet, C.: Sur un nouvel oxyde de rhénium: l'oxyde de rhénium (V), *Comp. Rend.* **261** (4) (1965) 1008-11.

[22] Borisova, L. V., Ryabchikov, D. I. and Yarinova, T. I.: Rhenium compounds in sulfuric acid solutions in the presence of reducing agents, *Zh. Neorg. Khim.* **13(2)** (1968) 321-8.

[23] Colaitis, D., Lebas, D. and Lecaille, C.: Un oxyde de rhénium en relation de structure avec V_2O_5, *Mater. Res. Bull.* **8**(6) (1973) 627-34.

[24] Varfolomeev, M. B. and Plyushchef, V. E.: Thermal stability of some rare earth perrhenates and yttrium, *Tsvetn. Metall.* **9** (1966), 98-101.

[25] Khrustalev, V. N., Varfolomeev, M. B., Shamrai, N. B., Struchkov, Y. T. and Pisarevskii, A. P.: Crystal structure of high-temperature modification of ytterbium perrhenate $Yb(ReO_4)_3$, *Koordinatsionnaya Khimiya* **19** (1993) 871-72.

[26] Baud, G. and Besse, J.-P.: Etude cristallochimique d'une nouvelle série d'oxides doubles de rhénium et de terres rares, *Mat. Res. Bul.*, **9** (1974) 1499-1502.

[27] Besse, J.-P., Bolte, M., Baud, G. and Chevalier, R.: Structure Cristalline d'Oxydes Doubles de Rhénium I. Sm_3ReO_8, *Acta Cryst.* **B32** (1976) 3045-48..

[28] Baud, G., Besse, J.-P., Chevalier, R. and Gasperin, M.: Structure cristalline de La_3ReO_8, *J. Solid State Chem.* **29** (1979) 267-72.

[29] Baud, G., Besse, J.-P. and Chevalier, R.: Les differentes formes cristallines de Y_3ReO_8. Relations avec la structure fluorine, *J. Solid State Chem.* **38** (1981) 186-91

[30] Rae-Smith, A. R., Cheetham, A. K. and Fuess, H.: Preparation and Crystal Structure of La_3ReO_8, *Z. anorg. allgem. Chem.* **510** (1984) 46-50.

[31] Kurbanov, T. K. and Mirishli, F. A.: Synthesis and study of new rhenium-containing crystals, *Azerb. Khim. Zh.*, **2** (1974), 119-21.

[32] Aitken, E. A., Bartram, S. F. and Juenke, E. F.: Crystal Chemistry of the Rhombohedral $MO_3 \cdot 3R_2O_3$ Compounds, *Inorg. Chem.*, **3** (1964) 949-54.

[33] Torardi, C. C. and Sleight, A. W.: Preparation and Crystal Structure of $La_3Re_2O_{10}$: An Example of Metal-Metal Bonding within Re_2O_{10} Units, *J. of the Less-Common Metals* **116** (1986) 293-99.

[34] Wilhelmi, K.-A., Lagervall, E. and Muller, O.: On the Crystal Structure of $Nd_4Re_2O_{11}$, *Acta Chem. Scand.* **21** (1970) 3406-8.

[35] Wltschek, G., Paulus, H., Svoboda I., Ehrenberg, H. and Fuess, H.: Crystal structure and magnetic properties of Sm_3ReO_7, *J. Solid State Chem.* **125** (1996), 1-4.

[36] Savel'eva, A. D., Varfolomeev, M. B., Fomichev, V. V. and Petrov, K. I.: Infrared Spectroscopic and X-Ray Diffraction Studies of the Family of Isotypical Compounds Ln_2ReO_5 (where Ln is Gd-Lu or Y), *Russian Journal of Inorganic Chemistry* **22** (1977) 1628-30.

[37] Baud, G., Besse, J.-P., Chevalier, R. and Gasperin, M.:Synthesis and structural study of the double oxide $Dy_5Re_2O_{12}$, *Mater. Chem. Phys.* **8** (1983) 93-99.

[38] Heumannskämper, D. H. and Jeitschko, W.: $Ho_5Re_2O_{12}$, *Z. Krist.* **178** (1987) 99.

[39] Besse, J.-P., Baud, G. and Chevalier, R.: Structure Cristalline d'Oxydes Doubles de Rhénium. II. L'Oxyde de Lanthane-Rhénium $La_6Re_4O_{18}$, *Acta Cryst.* **B34** (1978) 3532-35.

[40] Heumannskämper, D. H. and Jeitschko, W.: $Sm_3Re_2O_9$ and Eu_2ReO_5 mit Re-Re-Dreifachbindung, *Z. Krist.*, **182** (1988), 132-33.

[41] Longo, J. M. and Sleight, A. W.: Characterization and Structure of $La_4Re_6O_{19}$, a New Metal Cluster Compound, *Inorg. Chem.*, **7** (1968) 108-111.

[42] Morrow, N. L. and Katz, L.: The Crystal Structure of Lanthanum Rhenium Oxide, $La_4Re_6O_{19}$, *Acta Cryst.* **B24** (1968) 1466-71.

[43] Sleight, T. P., Hare, C. R. and Sleight, A. W.: Metal-Metal Bonding in $La_4Re_6O_{19}$ and Rutile-Related Dioxides, *Mat. Res. Bull.* **3** (1968) 437-44.

[44] Bramnik, K. G., Abakumov, A. M., Shpanshenko, R. V. Antipov, E. V. and Van Tendeloo, G.: Synthesis and Structure of $Ln_4Re_{6-x}O_{19}$ (Ln = Ce, Pr, Nd) Complex Oxides, *J. Alloys Comp.*, **278** (1998) 98.

[45] Muller, O. and Roy, R.: A Crystal Structure of Some New Rare Earth-Rhenium Oxides, *Mat. Res. Bull.* **4** (1969) 349-60.

[46] Waltersson, K.: The Crystal Structure of $La_4[Re_2]O_{10}$, a Fluorite-Related Structure Containing Rhenium Doublets, *Acta Cryst.* **B32** (1976) 1485-89.

[47] Wltschek, G., Paulus, H., Svoboda, I., Ehrenberg, H. and Fuess H.: Crystal structure and magnetic properties of Sm_2ReO_5, *J. Solid State Chem.* **132**, (1997) 196.

[48] Jeitschko, W., Heumannskaemper, D.H., Schriewer-Poettgen, M.S. and Rodewald, U.C.: Preparation, crystal structures, and properties of rhenates with multiple Re - Re bonds: Ln_2ReO_5 (Ln = Sm, Eu, Gd), $Ln_3Re_2O_9$ (Ln = Pr, Nd, Sm), and $Ln_4Re_6O_{19}$ (Ln = La Nd), *Journal of Solid State Chemistry*, **147** (1999) 218-28.

[49] Mujica, C., Gutiérrez, D., Llanos, J. and Cardoso, R.: Synthesis and crystal structure of Eu_2ReO_5, a complex oxide with Re-Re pairs in a tetragonal antiprismatic coordination, *J. Alloys Comp.*, **307** (2000) 127-30.

[50] Baud, G. and Capestan, M.: Composés oxygènes du rhénium(IV) et du lanthane. *Bull. Soc. Chim. Fr.*, **10** (1968) 3999-4004.

[51] Wltschek, G.: Dissertationsschrift, Fachbereich Chemie TU Darmstadt, 1994.

[52] Hartmann, T.: Diplomarbeit, Fachbereich Chemie TU Darmstadt, 1997.

[53] Hartmann, T., Ehrenberg, H., Miehe, G., Wltschek, G. and Fuess, H.: Preparation and characterization of rare earth-rhenium-oxides Ln_6ReO_{12}, Ln = Ho, Er, Tm, Yb, Lu, *J. Solid State Chem.* **148** (1999) 220-23.

[54] Bartram, S. F.: Crystal Structure of the Rhombohedral $MO_3 \cdot 3R_2O_3$ Compounds (M = U, W, or Mo) and Their Relation to Ordered R_7O_{12} Phases, *Inorg. Chem.*, **5** (1966) 749-57.

[55] Jeitschko, W., Heumannskämper, D. H., Rodewald, U. C. and Schriewer-Poettgen, M. S.: Preparation and Crystal Structure of Rare Earth Rhenates: the Series $Ln_5Re_2O_{12}$ with Ln=Y, Gd-Lu, and the Praseodymium Rhenates Pr_3ReO_8, $Pr_3Re_2O_{10}$, and $Pr_4Re_2O_{11}$, *Z. Anorg. Chem.* **626** (2000), 80-88.

[56] Ehrenberg, H., Hartmann, T., Wltschek, G., Fuess, H. Morgenroth, W. and Krane, H.-G.: The crystal structure of $Tm_5Re_2O_{12}$, *Acta Cryst.* B**55** (1999) 849-52.

[57] Blessing, R. H., *Acta Cryst.* **A51** (1995) 33-38.

[58] Sheldrick, G. M., SHELXL97. Program for the Refinement of Crystal Structures. University of Göttingen, Germany.

[59] Sheldrick, G. M., *Acta Cryst.* **A46** (1990) 467-73.

[60] Torardi, C. C., Fecketter, C., McCarroll, W. H. and DiSalvo, F. J.: Structure and Properties of $Y_5Mo_2O_{12}$ and $Gd_5Mo_2O_{12}$: Mixed Valence Oxides with Structurally Equivalent Molybdenum Atoms, *J. Solid State Chem.* **60** (1985) 332-42.

[61] Ehrenberg, H., Knapp, M., Hartmann, T., Fuess, H. and Wroblewski, T.: Resonant X-ray diffraction using high-resolution image-plate data, *J. Appl. Cryst.* **33** (2000) 953-57.

[62] Waseda, Y.: *Novel Application of Anomalous (Resonance) X-ray Scattering for Structural Characterization of Disordered Materials.* Heidelberg, Springer-Verlag (1984).

[63] Rodriguez-Carvajal, J.: *Abstracts of the Satellite Meeting of the XV. Congress of the International Union of Crystallography, Toulouse* (1990), 127.

[64] Chernaya, T.S., Muradyan, L.A., Rusakov, A.A., Kaminskii, A.A. and Simonov, V.I.: Refinement and analysis of atomic structures of $Er_3Al_5O_{12}$ and $(Y_{2.80}Er_{0.20})Al_5O_{12}$, *Kristallografiya*, **30** (1985) 72-75.

[65] Etschmann, B.E., Strel'tsov, V.A., Ishizawa N. and Maslen E.N.: Synchrotron X-ray study of $Er_3Al_5O_{12}$ and $Yb_3Al_5O_{12}$ garnets, *Acta Cryst.* **B57** (2001) 136-41.

[66] Shannon, R.D., *Acta Cryst.*, **A32** (1976) 751.

[67] Larson, A.C. and Dreele, R.v., GSAS – General Structure Analysis System, LANSCE, MS-H805, Los Alamos, National Laboratory Los Alamos, NM 87545 USA.

[68] X-STEP32, STOE & Cie GmbH, Darmstadt, 2000.

[69] Ehrenberg, H., Hartmann, T., Bramnik, K.G., Miehe, G. and Fuess, H.: Yttrium rhenium oxide Y_7ReO_{14}: a cubic fluorite superstructure, *Solid State Sciences* **6** (2004) 247 -50.

[70] Hartmann, T., Ehrenberg, H., Miehe, G., Buhrmester, T., Wltschek, G., Galy, J. and Fuess, H.: Preparation and crystal structure of Re_3O_{10}, *J. Solid State Chem.*, **160** (2001) 317-21.

[71] Hanawa, M., Muraoka, Y., Tayama, T., Sakakibara, T., Yamaura, J. and Hiroi, Z.: *Phys. Rev. Lett.* **87** (2001) 187001.

[72] Allan, Ph.B. and Schulz, W.W.: Bloch-Boltzmann analysis of electrical transport in intermetallic compounds: ReO_3, $BaPbO_3$, $CoSi_2$ and Pd_2Si, *Phys. Rev.* **B47** (1993) 1434-39.

Diese Arbeit wurde im Fachbereich Material- und Geowissenschaften der Technischen Universität Darmstadt unter der Leitung von Prof. Dr. H. Fueß in der Zeit vom 01.05.1998 bis 30.04.2003 durchgeführt.

Herrn Prof. Dr. H. Fueß danke ich für die interessante Themenstellung, seine großzügige Förderung, stete Gesprächsbereitschaft und langwährende Geduld.

Herrn Dr. Helmut Ehrenberg danke ich für seine uneingeschränkte Unterstützung, ständige Diskussionsbereitschaft, seine Hilfe bei den Messungen am B2 und bei der Auswertung der SQUID Messungen sowie seine konstruktive Kritik.

Herrn Dr. Gerhard Miehe danke ich für seine hilfsbreite Unterstützung bei der Lösung selbst der kniffeligsten Kristallstrukturen und der Auswertung der TEM Aufnahmen.

Herrn Dr. Michael Knapp danke ich ebenfalls für die gute Betreuung am B2. Ihm, Dr. Carsten Bähtz sowie Frau Dr. Christina Roth danke ich ferner für eine stets gute Atmosphäre und permanente Diskussionsbereitschaft.

Herrn Dr. Gernot Wltschek und Herrn Dr. Kirill Bramnik danke ich für so manche angeregte Diskussion in Sachen Rheniumchemie.

Herrn Dr. Winfried Kockelmann danke ich auf diesem Wege nochmals für die Messung der Neutronenpulverdiffraktogramme.

Ferner möchte ich stellvertretend für alle anderen Mitarbeiter des Fachgebiets Strukturforschung Herrn Dipl.-Ing. H. Mohren, Frau Ingrid Svoboda und Jean-Christophe Jaud für ihren Beitrag zum Gelingen dieser Arbeit danken.

Der Deutschen Forschungsgemeinschaft danke ich für die finanzielle Unterstützung dieser Arbeit (FU 125-33).

Publikationsliste

Hartmann, T., Ehrenberg, H., Miehe, G., Wltschek, G. and Fuess, H.: Preparation and characterization of rare earth-rhenium-oxides Ln_6ReO_{12}, Ln = Ho, Er, Tm, Yb, Lu, *J. Solid State Chem.* **148** (1999) 220-23.

Ehrenberg, H., Hartmann, T., Wltschek, G., Fuess, H. Morgenroth, W. and Krane, H.-G.: The crystal structure of $Tm_5Re_2O_{12}$, *Acta Cryst.* B**55** (1999) 849-52.

Ehrenberg, H., Knapp, M., Hartmann, T., Fuess, H. and Wroblewski, T.: Resonant X-ray diffraction using high-resolution image-plate data, *J. Appl. Cryst.* **33** (2000) 953-57.

Lampakis, D., Palles, D., Liarokapis, E., Panagopoulos, C., Cooper, J.R., Ehrenberg, H: and Hartmann, T.: Phase Transitions and Raman Spectra Correlations in $La_{2-x}Sr_xCuO_4$ ($0 \leq x \leq 0.45$), *Phys. Rev. B.* **62** (2000) 8811-17.

Hartmann, T., Ehrenberg, H., Miehe, G., Buhrmester, T., Wltschek, G., Galy, J. and Fuess, H.: Preparation and crystal structure of Re_3O_{10}, *J. Solid State Chem.* **160** (2001) 317-21.

Kniep, R., Koch, D., and Hartmann, T.: Crystal structure of potassium aluminium catena-(monohydrogenmonoborate)-bis(monophosphate), $KAl[BP_2O_8(OH)]$, *Z. Kristallogr. NCS* **217** (2002) 187.

Ehrenberg, H., Hartmann, T., Bramnik, K.G., Miehe, G. and Fuess, H.: Yttrium rhenium oxide Y_7ReO_{14}: a cubic fluorite superstructure, *Solid State Sciences* **6** (2004) 247-50.

Tagungsbeiträge

Jahrestagung der Deutschen Gesellschaft für Kristallographie 1998, Karlsruhe: Hartmann, T., Ehrenberg, H., Miehe, G., Wltschek, G, Fuess, H.: Preparation and characterization of new rare earth-rhenium oxides Ln_6ReO_{12}, *Z. Kristallogr. Suppl. Issue No* **15** (1998) 31.

High-temperature superconductors and novel materials, HTSC-V, Moscow, 1998: Hartmann, T., Ehrenberg, H., Miehe, G. Wltschek, G., Fuess, H.: Physical Properties of Crystalline Phases in the System $Ln_2O_3 – ReO_2 – Re_2O_7$.

18. European Crystallographic Meeting 1998, Prague: Ehrenberg, H., Hartmann, T., Wltschek, G. Doyle, R., Fuess, H.: Crystal structure and physical properties of compounds in the phase system $Ln_2O_3 – ReO_2 – Re_2O_7$, *Materials Structure in Chemistry, Biology, Physics and Technology* **Vol. 5**, special issue, page 82 (ISSN 1211-5894).

XVIIIth International Union of Crystallography Congress 1999, Glasgow: Hartmann, T., Ehrenberg, H., Miehe, G., Buhrmester, T., Wltschek, G., Fuess, H.: Crystal structure of a new binary rhenium oxide Re_3O_{10}.

Jahrestagung der Deutschen Gesellschaft für Kristallographie 2000, Aachen: Hartmann, T., Ehrenberg, H., Miehe, G., Wltschek, G, Knapp, M., Fuess, H.: $(Y,Re)O_2$: ein Fluorit-Abkömmling im System $Ln_2O_3 – ReO_2 – Re_2O_7$.

7. European Powder Diffraction Conference, 2000, Barcelona: Ehrenberg, H., Hartmann, T., Knapp, M., Miehe, G., Wltschek, G., Fuess, H., Svoboda, I., Kockelmann, W.: Fluorite superstructures in rare-earth rhenium oxides.

Jahrestagung der Deutschen Gesellschaft für Kristallographie 2001, Bayreuth: Ehrenberg, H., Knapp, M., Hartmann, T., Bähtz, C., Svoboda, I., Fuess, H., Schmidt, H., Krane, H.-G.: Die Kristallstruktur von Dy_3ReO_8, *Z. Kristallogr. Suppl. Issue No* **18** (2001) 123.

14te Deutsche Zeolithtagung, 2002, Frankfurt am Main: Stock, N., Bauer, S., Hartmann, T., Baumgartner, B., Bein, T.: Automated Parallel Synthesis and Characterization of Microporous Materials.

Lebenslauf

Name:	Thomas Hartmann
Adresse:	Ehretstr. 15 64285 Darmstadt
Geburtsdatum:	11.02.1968
Geburtsort:	Solingen

Schule und Beruf:

1974 – 1978	Grundschule: Heinrich-Heine-Schule, Darmstadt
1978 – 1987	Gymnasium: Lichtenbergschule, Darmstadt
1987 – 1995	Studium der Chemie an der Technischen Hochschule Darmstadt
1996	Wehrdienst
11/1996 - 5/1997	Abschluss Diplomarbeit über „Darstellung und Untersuchung von neuen Seltenerd-Rhenium-Oxiden Ln_4ReO_8 und Ln_6ReO_{12}“
10/1997 - 4/1998	Studentische Hilfskraft mit Abschluss im Fachgebiet Strukturforschung, Fachbereich Materialwissenschaft, Technische Universität Darmstadt
5/1998 – 12/2000	Wissenschaftlicher Mitarbeiter im Fachgebiet Strukturforschung, Fachbereich Materialwissenschaft, Technische Universität Darmstadt
seit 1/2001	Angestellter der Firma STOE & Cie GmbH, Darmstadt

Eidesstattliche Erklärung

Hiermit erkläre ich an Eides statt, dass ich meine Dissertation selbständig und nur mit den angegebenen Hilfsmitteln angefertigt und noch keinen Promotionsversuch unternommen habe.

Darmstadt, den